CHARACTERIZATION OF NHLRC2 GENE-EDITED MICE: A MODEL FOR BOVINE DEVELOPMENTAL DUPLICATIONS

BY

JOCELYN DENAE DELHOTAL

THESIS

Submitted in partial fulfillment of the requirements
for the degree of Master of Science in Animal Sciences
in the Graduate College of the
University of Illinois at Urbana-Champaign, 2016

Urbana, Illinois

Master's Committee:

Professor Jonathan E. Beever, Chair
Assistant Professor Anna C. Dilger
Professor Matthew B. Wheeler

Abstract

Developmental duplications (DD) is a genetic condition recently characterized in Angus cattle. It is a congenital abnormality where duplication of neural crest derived tissues occurs during embryonic development. A common phenotypic presentation of the condition includes calves born with polymelia most frequently involving duplication of the front limbs that protrude from the neck or shoulder region. Aside from polymelia, DD affected individuals present malformations associated with neural tube defects (NTDs). Genome-wide association studies have identified a single locus associated with this disease phenotype. Further investigation has identified the putative mutation as a nonsynonymous substitution (p.Val311Ala) in the NHL repeat-containing 2 (*NHLRC2)* gene. Transcription activator-like effector nucleases (TALENs) targeting exon 5 of *NHLRC2* were used for gene-editing of the orthologous locus in mice to further investigate the role of *NHLRC2* in development. Three mouse lines were generated with mutations having varying impacts on the *NHLRC2* protein. Two mutations, -2 bp and -19 bp, are predicted to cause a prematurely truncated protein and one mutation, -12 bp, the deletion of four amino acids, residues 307 through 310, adjacent to the corresponding bovine substitution. Heterozygous mice of each line were intermated to phenotypically characterize homozygous progeny. Genotyping of the offspring revealed absence of homozygous individuals suggesting embryonic lethality. Because initiation of neural tube closure in mice occurs at day E8.5, embryonic death was assessed at this developmental day by harvesting embryos from heterozygous matings at day E8.5 with subsequent genotyping. Again, no homozygous embryos could be detected, however yolk sacs containing no embryos were observed. Furthermore, the number of yolk sacs exceeded the average number of live births by 68% (11.3 vs. 6.7), indicating embryonic lethality of homozygous individuals most likely occurs between fertilization and

E8.5. Thus, we suggest that *NHLRC2* is essential during mammalian development and hypothesize *NHLRC2* plays a significant role in neurulation.

Table of Contents

Chapter 1: Literature Review

1.1 Using Gene Mapping to Understand Phenotypes

Knowledge about how specific genes influence mammalian development began in the early 1900s with experiments on the inheritance of coat colors in a variety of domestic animals (Hogan, Costantini, & Lacy, 1994). In 1903, the Boveri-Sutton chromosome theory was established, further clarifying Mendelian laws of inheritance by demonstrating chromosomes were central to genetic inheritance (Sturtevant, 1913). Shortly after, Thomas Hunt Morgan confirmed the chromosome theory through his observation of different traits within fruit flies, such as eye color and body color, making Morgan the first person to link trait inheritance to a specific chromosome (Miko, 2008). This led Alfred Sturtevant to determine the relative location of genes to one another on a chromosome and to generate the first genetic map of a chromosome (Sturtevant, 1913). Thus, genetic mapping is a powerful approach to identify chromosomal locations of genes influencing variation in phenotypic traits. Furthermore, it can facilitate a better understanding of the complex genetic organization of organisms. Approaches for mapping include methods such as linkage mapping and physical mapping. Although many biological mechanisms of simple, single gene phenotypes remain unknown, the advancement of mapping techniques and marker types continue to aid in connecting specific phenotypes to genotypes.

Preceding the knowledge of DNA sequences of genes, the location of genes could be mapped to specific chromosomes by tracking transmission in family pedigrees of specific phenotypes associated with different alleles of the same gene (Chial, 2008). The first genetic maps used visual phenotypes as markers, with the only possible studies consisting of genes that correlated with these phenotypes (Brown, 2002). Sturtevant (1913) discovered the chance of recombination, or the exchange of DNA segments during meiosis, is related to the distance

between genes. Linkage analysis then estimates the distance between genetic loci and relies on the fact that genes near one another on a chromosome are likely to be inherited together. Two genes that are close together on a chromosome will be separated by recombination less frequently than genes that are farther apart. Therefore, recombination frequency is proportional to the relative distance between genes, leading to the capability of producing a linear map of genes along a chromosome. However, linkage mapping requires pedigree information in order to observe co-segregation or the tendency for linked genes to be inherited together. These early maps also lacked resolution, containing large uncharacterized genomic regions. These gaps consisted of genes without an associated phenotype, thus lacking the ability to be mapped.

Because not all genes correlate with a visual phenotype, the discovery of DNA markers permitted great improvement in genetic mapping and genome characterization. DNA markers identify variation within an organism's DNA sequence, producing a more comprehensive genetic map without the need for phenotypic variation. Restriction fragment length polymorphisms (RFLPs) were one of the first DNA markers implemented as part of the Human Genome Project. RFLPs are the result of a variation or polymorphism within a DNA sequence leading to a change in a restriction enzyme recognition site. DNA restriction enzymes recognize specific sequences and cleave the DNA molecules into fragments. A polymorphism within a restriction site results in sites that can no longer be cleaved by its restriction enzyme. Therefore, a sequence variation in restriction sites between homologous DNA sequences can be detected by their different fragment lengths after digestion with a specific restriction endonuclease (Botstein, White, Skolnick, & Davis, 1980). The RFLP assay, however, is time consuming and labor intensive, with few loci detected per assay (Powell et al., 1996).

Microsatellites soon became the marker of choice, being the first to take advantage of Polymerase Chain Reaction (PCR) (Zietkiewicz, Rafalski, & Labuda, 1994). Microsatellites are short segments of DNA that contain a di, tri or tetranucleotide repeat also known as simple sequence repeats (SSRs; Weber and May, 1988). They are abundant and fairly evenly distributed within an organism's genome (Litt & Luty, 1989). Each locus is adjacent to a unique sequence and can be complimented by specific primers for use in the amplification of the microsatellite locus by PCR. Making use of PCR technology, microsatellites improved the speed of genetic mapping (Weber & May, 1989). However, use of these markers requires flanking sequence information. Also, microsatellite markers developed for one species exhirbit less homology across same or different taxa (Roa et al., 2000).

Currently, single-nucleotide polymorphisms (SNPs) are the marker of choice when it comes to genetic mapping. SNPs differ by one or more nucleotides among individuals of the same species (Alberts et al., 2002). These polymorphisms have been characterized since the beginning of DNA sequencing, but their ability to be rapidly genotyped in large numbers came about with the advancement of high-throughput SNP technology platforms (Chee Seng, Katherine, & Kee Seng, 2001). SNPs are currently widely used on any size scale due to their abundance within genomes and their ability to identify polymorphisms missed by other markers (I. C. Gray, Campbell, & Spurr, 2000). Therefore, using SNPs as markers lead to an increase in mapping efficiency (Hoskins et al., 2001).

It was first shown by Risch and Merikangas (1996) that performing an association scan of one million variants in a genome within samples of unrelated individuals had the potential to be more effective than conducting linkage analysis with only a few hundred markers. They argued that the linkage analysis method had limited power in detecting genes of modest effect and an

association study approach utilizing candidate genes would give a greater outcome. The experimental design of genome wide association studies (GWAS) has led to new discoveries about genes and pathways involved in common diseases and traits. These studies are aimed at detecting variants at genomic loci that associate with complex traits within populations. This approach involves rapidly scanning markers across genomes of many individuals to find genetic variations, particularly SNPs, associated with the disease of interest (Norrgard, 2008). They are based upon the principle of linkage disequilibrium at the population level (Visscher, Brown, McCarthy, & Yang, 2012). Genome-wide association studies have resulted in detection of hundreds of common variants whose allele frequencies correlate with various illnesses, traits, and phenotypes continuing to provide the scientific community with an abundance of new biological information for clinical utilization (McClellan & King, 2010).

1.2 Developmental Duplications Phenotypes

Developmental duplications (DD) is a congenital autosomal recessive condition recently characterized in cattle. Phenotypic presentations of affected calves consist of anatomic duplications derived from neural crest tissues. Specifically, phenotypes of DD consist of various forms of polymelia as well as neural tube defect malformations. Polymelia is also referred to as supernumerary, or extra limbs, and is often associated with other congenital defects such as polydactyly and the addition of often underdeveloped bones (Muirhead, Pack, & Radtke, 2014). There are many different forms of polymelia, each classified by the point of attachment to the body (L. Denholm, 2011). Notomelia consists of attachment of the additional limbs in the embryonic notochord region, cephalomelia is attachment to the head, thoracomelia is on the thorax below the dorsal midline, and dipygus, also known as pygomelia, is attachment to the

pelvic region. The extra limb can develop as a forelimb or hindlimb and have either a left or right side anatomy. It is not uncommon for an affected individual to have more than one supernumerary limb. In most cases however, the extra limb is shorter and consists of no muscle mass (L. Denholm, 2011). Polymelia poses a significant economic impact due to losses from dystocia and the high costs associated with amputation in affected calves that survive birth. Many calves with this condition appear to grow and breed normally despite removal or maintenance of the supernumerary limbs (L. Denholm, 2011).

Aside from polymelia, DD affected individuals present with congenital malformations that are associated with neural tube defects (NTDs). NTDs are the second most common group of birth defects among humans (Wallingford, Niswander, Shaw, & Finnell, 2013). NTDs are characterized by disruption of early embryonic events during central nervous system formation that result in failure of neural tube closure. There are a variety of malformations classified under the general description of NTDs, with a wide range of clinical severity. Among severe NTDs affecting brain development, cases of open lesions of the brain have been observed in DD affected individuals, often lethal at or before birth (Copp and Greene 2013). Lethality is a result of the failure of primary neurulation and is characterized by bending of the neural plate and closure of the neural tube in the dorsal midline (Gilbert, 2000). Closed spine lesions are less severe, sometimes even asymptomatic, often occurring in the low sacral and coccygeal region during secondary neurulation that generates the secondary neural tube (Murdoch et al., 2014). Among spinal cord malformations, cases of sacral spina bifida along with its severe form of myelomeningocele and associated spinal cord tethering, butterfly vertebrae and split cord malformation have been observed in DD affected individuals (L. J. Denholm et al., 2016).

Tumor-like cases include spinal embryonic teratoma, sacral and occipital myolipoma, dermoid cysts and dermoid sinus. Other NTD phenotypes with DD consist of twinning defects such as heteropagus rachipagus and conjoined twins, craniofacial dysmorphogenesis and micropthalmia as well as gastrochisis. Both genetic and non-genetic factors are known contributors in the development of NTDs with up to 70% being genetically attributed (Andrew J. Copp & Greene, 2013). However, the precise contribution of genetic factors such as function, number, or prevalence in affected individuals is still largely undiscovered for specific risk genes. The various NTD phenotypes associated with DD affected individuals will aid in further understanding the role genes have in NTDs in general.

1.2.1 Mammalian Neurulation and Key Signaling Pathways

Neurulation results in formation of the neural tube, the precursor of the brain and spinal cord and ultimately forms the central nervous system (Andrew J. Copp, Greene, & Murdoch, 2003). This is an intricate process that involves many diverse cellular functions and chemical pathways (Sadler, 2005). Due to its complexity, the neurulation process can be interrupted at several key developmental time points, resulting in neural tube defects. Neurulation is broken down into a two-stage progression within birds and mammals, known as primary and secondary neurulation. It develops in a cranial to caudal, or head to toe, direction without any interaction between the two stages (A. J. Copp & Brook, 1989).

Primary neurulation involves the formation of the neural tube between the forebrain and caudal neuropore, or the opening that forms during folding of the neural tube (Morriss-Kay, Wood, & Chen, 2007). According to Schoenwolf and Smith (2000), primary neurulation occurs in four stages; 1) initiation by the formation of the neural plate, 2) shaping of the neural plate, 3)

bending and fusion of the neural folds and 4) neural groove closure (Figure 1.1). These stages occur simultaneously, each in their own anatomical region. Ectodermal thickening caused by the change in cuboidal to columnar epithelial cells results in the formation of the neural plate (Purves, Augustine, Fitzpatrick, & et al., 2001). The neural plate is then shaped by narrowing and extending, otherwise known as convergent extension, as well as continued thickening (Zohn & Sarkar, 2008). The planar cell polarity (PCP) pathway, a non-canonical WNT signaling cascade, is required for the shaping stage (Massa et al., 2009). The bending of the neural plate requires formation of hinge points, neural folds, and neural plate folding and is regulated by the sonic hedgehog (Shh) signaling pathway as well as bone morphogenetic protein signaling (Andrew J. Copp, et al., 2003; Massa, et al., 2009). According to Gilbert (2000), two types of hinge points form during neural plate bending, the medial and dorsal lateral hinge points. The hinge regions are where the neural tube comes into contact with adjacent tissue. The movement of cells around the hinge points forms bilaminar folds, their inner layer containing the neural plate and an outer layer of epithelial ectoderm. These neural folds then ascend with the help of the medial hinge point, and pair with dorsal lateral hinge points. As a result of bending, the neural folds begin to align at the dorsal midline and with signaling from the PCP pathway, neural tube closure is initiated (Andrew J. Copp, et al., 2003; Sadler, 1978). Neural tube closure is initiated at several points along the rostrocaudal axis in mammals and birds (Yamaguchi & Miura, 2013). The folds adhere to one another and merge together, creating a tube like structure, hence the term neural tube. Surface epidermal ectoderm formerly bordering the neural plate then encases the newly formed neural tube (Oppenheim & Haverkamp, 1986). This primary neurulation stage results in the development of the brain and most of the spinal cord.

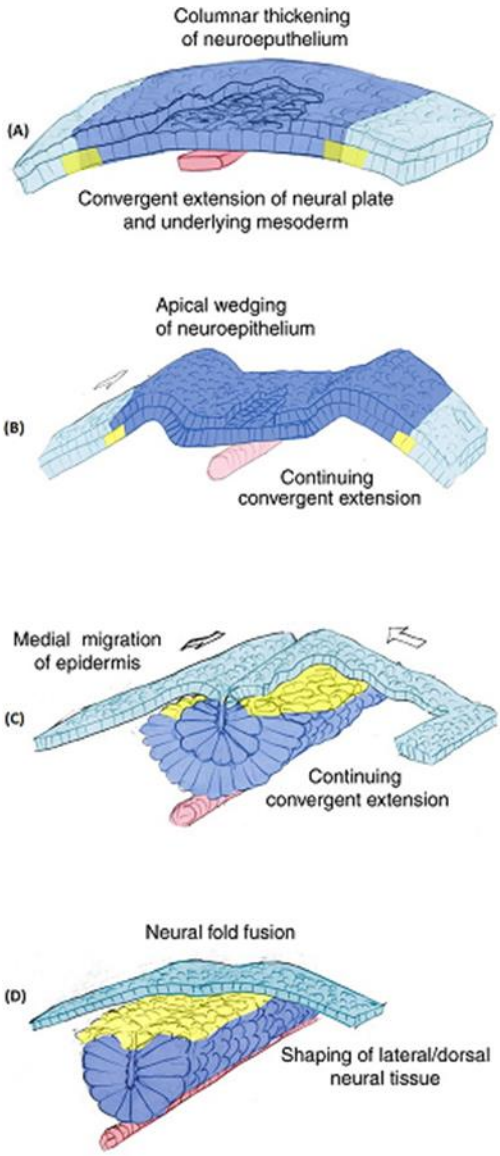

Figure 1.1 Primary Neurulation. (A) The neural plate is formed by the change in cuboidal to columnar epithelial cells. The neural plate is shaped by convergent extension movements while neuroepithelium continues to thicken requiring the PCP pathway. (B) The neural folds begin to ascend and pair with dorsal lateral hinge points. (C) Neural folds converge at the dorsal midline. (D) Neural folds adhere to one another and create a tube like structure. Neuroepithelium, blue; dorsal neural tissue and neural crest, yellow; epidermis, light blue; notochord, red. (Image adapted from (Wallingford & Harland, 2002).

Occurring at the future base of the spine, the transition between primary and secondary neurulation begins (Andrew J. Copp & Greene, 2013). According to Copp (2003), secondary neurulation is formed within the tail bud, or lowest spinal region, without the need for neural folding. The tail bud is composed of a self-renewing stem cell population that is left after the primitive streak diminished. The primitive streak consists of a band of cells that form during early gastrulation, also known as a precursor for neural tube development (Gilbert, 2000). These

cells proliferate rapidly and contribute to the longitudinal development of the body axis, becoming the main source for all non-epidermal tissues, including the neural tube and vertebrae. The guided movement of mesenchymal cells from the tail bud create the secondary neural tube, forming a continuous lumen within the primary neural tube (Zohn & Sarkar, 2008). This process results in the formation of the lowest section of the spinal cord.

The bending and shaping of the neural plate that is necessary to complete the neural tube is thought to be dependent upon cranial neural crest cell migration (Andrew J. Copp, et al., 2003). According to Hogan et al. (1994), the neural crest is a population of cells originating in the dorsal part of the neural tube. Crest cells migrate away from the neural tube to ventral and dorsolateral locations to become a wide variety of cell types based on their axial location. In the midbrain and hindbrain, crest cells detach from the neural folds and begin to migrate before the initiation of neural tube closure (Yamaguchi & Miura, 2013). However, in the spinal, or lower region, neural crest cell migration begins hours after the completion of neural tube closure (Andrew J. Copp, 2005).

Programmed cell death, also known as apoptosis, plays an important role in animal development such as removing cells between digits as well as being involved in the hollowing of structures creating cavities (Jacobson, Weil, & Raff, 1997). A study conducted by Schluter (1973) observing mouse embryos under an electron microscope for zones of cell death, first provided evidence that cell death within the neuroepithelium during neurulation is programmed. In 1993, the role of caspase enzymes in apoptosis was discovered, cleaving one another and key intracellular proteins in order to execute cells in a controlled manner (McIlwain, Berger, & Mak, 2013). Weil et al. (1997) suppressed apoptosis in developing chick embryos by inhibiting caspases, resulting in the failure of neural tube closure, thus ultimately proving the requirement

of apoptosis during mammalian neurulation. Massa (2009) also investigated the role of apoptosis in neurulation and was able to show that it occurs mainly during the bending and fusion of the neural folds, post fusion remodeling of the neural tube, and migration of the neural crest cells away from the neural tube. This study also suggests that excess apoptosis could cause NTD development by causing a lack of cells needed in order to successfully complete neural tube closure. In mice, several KO strains with NTD development contain alterations in the normal amount of apoptotic cells. Most of these strains show an increase in cell death as well as having a few genetically determined mouse NTDs in connection with reduced apoptosis, further emphasizing the correlation between neurulation and apoptosis (Muriel J. Harris & Juriloff, 2007). Copp's (2003) neurulation review states that the neuroepithelium is also proliferative during neurulation, with cells beginning to leave the cell cycle and differentiate only after neural tube closure is complete at each point along the body axis. Excessive cell proliferation, however, has been identified in individuals with neural tube defects; leading to the conclusion that successful neurulation requires a balance between proliferation and differentiation of cells.

1.3 *NHLRC2*, the gene for developmental duplications

Bovine developmental duplications is caused by a mutation in the *NHL repeat containing* (*NHLRC2*) gene. *NHLRC2* is a protein coding gene with known and predicted orthologs in 181 organisms (Pruitt et al., 2014). In the mouse, *NHLRC2* is highly expressed within the nervous system (Smith CM et al., 2014). There is presently no known function of the NHLRC2 protein, but it has been shown to be linked to late-onset Alzheimer Disease in humans (Grupe et al., 2006). Currently, no mutations in the *NHLRC2* gene or associated phenotypes have been reported in any species other than cattle.

1.3.1 *NHLRC2* Gene Organization

NHLRC2 is located on bovine chromosome 26 and has 12 exons, spanning approximately 55.59 kb (NCBI Reference Sequence: NM_001083723.2). Bovine *NHLRC2* has one transcript and contains 726 amino acids (Herrero et al., 2016). Mouse *NHLRC2* is located on chromosome 19, with 11 exons, spanning 55.24 kb (NCBI Reference Sequence: NM_025811.3). Mouse *NHLRC2* also has one transcript and contains 725 amino acids (Pruitt, et al., 2014).

1.3.2 Related Gene Family Members

The *NHLRC2* gene is one of four NHL repeat containing proteins involved in protein-protein interactions and is named after the NCL-1, HTA and Lin-41 genes first discovered and named for the 2-6 repeats of an approximate 44-residue protein domain (Slack & Ruvkun, 1998). *NHLRC2* has a thioredoxin and 6-blade b-propeller TolB-like domain. Thioredoxins are major cellular protein disulfide reductases serving as electron donors for enzymes (Arnér & Holmgren, 2000). They also protect proteins from inactivation, help cells deal with stress, and regulate programmed cell death by removing nitric oxide elements, or denitrosylation (Collet & Messens, 2010).

1.3.2.1 *NHLRC1*

Although *NHLRC2* is not well characterized, *NHLRC1* has been shown to play a role in disease (Chan et al., 2003). *NHLRC1* is one of the four NHL repeat-containing protein family along with NHLRC2 (Pruitt, et al., 2014). *NHLRC1* is a single exon gene, having two transcripts (Chan, et al., 2003). *NHLRC1* is referred to as the NHL Repeat Containing E3 Ubiquitin Protein Ligase 1 (Singh & Ganesh, 2009). *NHLRC1* is predicted to produce a 395 amino acid protein

known as malin. Chan (2003) discovered *NHLRC1* as a causative gene, along with the previously discovered EPM2A gene, in the onset of the autosomal recessive Lafora disease (LD), a progressive and fatal neurodegenerative disorder also known as progressive myoclonic epilepsy type 2. Symptoms of LD include cognitive defects, myoclonic epilepsy, ataxia and dementia (Singh & Ganesh, 2009). These mutations result in the accumulation of the phosphatase laforin, that is otherwise normally polyubiquitinated by *NHLRC1* (Brackmann, Kiefer, Agaimy, Gencik, & Trollmann, 2011). Ubiquitination directs proteins for degradation through the proteosome, alters protein location, and affects protein activity and protein-protein interactions (Glickman & Ciechanover, 2002).

NHLRC1 mutations impair the encoded protein malin from normally degrading laforin (Brackmann, et al., 2011). This results in intracellular deposits of insoluble glycogen within neurons, thus making the degradation of laforin a key aspect in regulating cell death. A more recent study investigated the possible role the *NHLRC1* protein may have in the p53 mediated cell death pathway (Upadhyay, Gupta, Bhadauriya, & Ganesh, 2015). It was observed that loss of lafora or malin resulted in increased levels and activity of p53, a cell cycle regulator. This outcome is primarily due to the associated increased level of Hipk2, a proapoptotic activator of p53, suggesting overall that the activation of Hipk2-p53 cell death pathway may be the cause of cell death, or neurodegeneration as seen in Lafora disease.

1.3.2.2 *Slimb*

A genetic basis of supernumerary limbs is demonstrated in the *slmb* (supernumerary limbs) gene within the fruit fly *Drosophila melanogaster*. *Slmb* is one of three F-Box/WD40 repeat proteins with the *Drosophila* genome. WD repeat proteins resemble that of NHL repeats;

they are both known to be involved in protein-protein interactions, contain multiple repeat units and are of similar length (Neer, Schmidt, Nambudripad, & Smith, 1994). F-Box/WD40 proteins are subunits of a multi-protein complex and are components of E3 ubiquitin ligases, recruiting substrates such as cell cycle regulators in yeast and other substrates within mammals to the ubiquitin-dependent proteolytic system (L. Denholm, 2011; Kawakami et al., 2000). The ubiquitin-proteasome pathway consists of connecting ubiquitin polypeptides to proteins targeting them for degradation, making it an important pathway for protein regulation in eukaryotes (Lecker, Goldberg, & Mitch, 2006). The Interactive Fly database (2000) classified *slmb* as an important regulator of the Wingless (Wg), Hedgehog (Hh), and dorsal developmental pathways. Jiang and Struhl's (1998) review on *slmb* states that the gene is normally negatively regulated by both the Hh and Wg signal transduction pathways. Hh signal transduction leads to the increased stability of the patterning formation transcription factor *cubitus interruptus (ci)* and Wg signal transduction leads to increased stability of the cell adhesion *armadillo* (*arm*) gene (Fly, 1996; Peifer, Orsulic, Sweeton, & Wieschaus, 1993). Loss of function mutations within the *slmb* gene results in mutated cell accumulation of both *ci* and *arm* as well as abnormal expression of both the Hh and Wg responsive genes.

Jiang and Struhl (1998) classified the three *slmb* alleles; $slmb^{1}$ was observed to behave hypomorphically, causing partial loss in gene function, while $slmb^{2}$ and $slmb^{P1493}$ elimate most to all of *slmb*'s function, their mutant cells showing phenotypes attributed to abnormal Wg and Hh signal transduction. Wojcik (2000) later found that *slmb* is required in Drosophila neuroblasts to restrict centromere duplication during the cell cycle, emphasizing its role during central nervous system development. Theodosiou (1998) found *slmb* also regulates Wg and decapentapliegic, a key developmental morphogen, in both the anterior/posterior and dorsal/ventral axes. These

studies demonstrate the *slmb* gene being a key regulator in body pattern development within *Drosophila.* Although the function of *NHLRC2* is not well characterized, it has phenotypic characteristics like that of *slmb* suggesting these two genes have similar functions, being a key factor during development.

1.4 Use of a Mouse Model

Animal models are a valuable resource for studying orthologous diseases between species. Basic cell processes in most mammals are very similar due to their related anatomy. Thus, biological research using animal models facilitates our understanding of the development and function of organisms. Furthermore, the use of animals in research has significantly helped accelerate scientific progress and is a key contributor to the development of effective drugs, therapies and cures used today (Hau, 2008).

Rodents have been used in research for nearly a century and make effective models in research due to their well understood anatomy, physiology, and genetics (Hau, 2008). According to the Foundation for Biomedical Research, 95% of all laboratory animals are mice and rats (Melina, 2010). The mouse model in particular is a powerful research tool because of their cost effectiveness, in large part due to their size and rapid regeneration time. Mice have a 19-21 day gestation period and produce a relatively large litter size, with reproduction possible as often as every three weeks (Hogan, et al., 1994). They can also be highly inbred to yield identical individuals, allowing for uniformity within a research colony.

The mouse is also an excellent organism for genome manipulation. This makes it a well-known organism for generating disease models through manipulation of known causative genes (Spencer, 2002). The Jackson Laboratory, a top laboratory mouse distributor with the most

published mouse models in the world, currently maintains over 7,000 genetically defined strains of mice (Shultz, 2016). Models currently available for genetic research include mice prone to specific cancers, diabetes, obesity, blindness, Huntington's disease, anxiety, behavior, addiction, as well as many others.

Genetic mouse models have also been recognized to be an important tool when studying neural tube closure in mammals (J. Gray & Ross, 2011). NTD mouse models allow for the identification of neurulation genes by observing embryonic development. These mouse models provide an accommodating system for discovering the development, pathological and molecular mechanisms that bring about NTDs (Zohn & Sarkar, 2008). The current number of mouse mutants containing NTDs is more than 240, consisting of 205 with specific causative genes, 30 unidentified genes, and 9 multifactorial strains (Muriel J Harris & Juriloff, 2010).

1.4.1 Mouse Developmental Timeline

Mice are an effective research tool when investigating development due to their gestational period lasting a mere 19-21 days. Embryonic development begins with fertilization of the egg by the sperm, cleavage and blastulation occurs during embryonic days (E) 0-5; implantation, gastrulation and early organogenesis during E5-10.0, organogenesis occurs between E10-14.0, and the last period of fetal growth and development occurs between E14-19.0 (Hogan, et al., 1994). The first period that occurs encompasses from fertilization to implantation and is known as the preimplantation period (Wang & Dey, 2006). The success of preimplantation is dependent upon the degradation of maternal debris, activation of the embryo's genome, cell cycle progression ensuring appropriate initial cell lineages, as well as the formation of a blastocyst with subsequent implantation on the uterine wall (Li, Zheng, & Dean, 2010).

Beginning on E0.5, the embryo is composed of only one cell. By E1.5, the embryo is at the 2 cell stage and has initiated expression of its own genome (Hogan, et al., 1994). After the four cell stage on E2.0, the embryo continues to go through several mitotic cell divisions, forming a ball of cells that undergo compaction. These compacted cells are known as the morula and develop apical and basal membranes (top and bottom) (Marikawa & Alarcón, 2009). Upon compaction, a fluid-filled blastocoel cavity forms on E3.5 and becomes a blastocyst (Fong et al., 1998). The mature blastocyst is composed of three cell types: the outer epithelial trophectoderm, the primitive endoderm, and the pluripotent inner cell mass (ICM) (Wang & Dey, 2006).

Localization of the embryo ICM defines the polar and mural trophectoderm with the mural trophectoderm located opposite the ICM (Sutherland, 2003). On E4.5, implantation into the uterine wall of the fully formed blastocyst is initiated by the mural trophectoderm's connection with the luminal epithelium of the uterus (Li, et al., 2010). During implantation, there is an increase in endometrial vascular permeability at the site of blastocyst attachment (Zhang et al., 2013). Following the completion of implantation, there is a dramatic increase in the embryo's growth rate, specifically in the pluripotent cells of the epiblast or primitive ectoderm from which the fetus develops (Hogan, et al., 1994). Shortly after implantation, the anterior-posterior axis of the embryo is firmly established (E5.5) (Takaoka & Hamada, 2012).

Blastocyst attachment induces the formation of the uterine crypt and also stimulates formation of decidual tissue, a spongy mass of cells originating from the uterine stroma known as the decidual reaction (Zhang, et al., 2013). These cell masses around a single embryo are referred to as the deciduum, translating to 'that thing that falls off' (Hogan, et al., 1994). According to Palis (2006), gastrulation begins at E6.5 as mesodermal cells pass through the primitive streak to occupy a position between the primitive ectoderm and visceral endoderm

germ layers. At E7.0, mesoderm cells migrate to line the exocoelomic cavity and enter the embryo proper, eventually differentiating into the mature embryo. E7-7.5 marks the initiation of yolk sac formation. The yolk sac is a bilayer structure of mesoderm and endoderm derived cell layers that the survival of the embryo becomes dependent upon. In addition to the yolk sac, the development of the neural plate begins at E7-7.5. According to Gray and Ross (2011), neural tube closure begins at E8.5 at the hindbrain/cervical boundary prior to embryo turning. The conclusion of cranial neural fold and caudal neuropore closure occurs on E9.5, with cranial neurulation completed by E10.0 (Andrew J. Copp & Greene, 2013; J. Gray & Ross, 2011).

Hogan (1994) states that forelimbs begin appearing at E9.0 with hind limbs becoming detectable at E10. Bone and cartilage elements for limbs are derived from the lateral mesoderm of the initial outgrowth and the limb musculature initiates from myotome cells migrating from the somite into the limb bud at a later stage. As limb bud growth continues, the surface ectoderm overlying the distal tip thickens into the apical ectodermal ridge (AER), essential for maintaining proliferation and patterning of the underlying progress zone (PZ). Anterior/posterior patterning of the limbs requires the zone of polarizing activity (ZPA). Members of the *Hox* gene family (A and D) that control an embryo's body plan along the head to tail axis, are expressed in a region specific manner within the limb. Cartilage formation in the developing embryo is complete on E12.5 and bone formation complete by E15.0 (Hogan, et al., 1994). Fetal growth development is the final stage during gestation, occurring from E14.0 until birth.

1.4.2 Bovine developmental timeline

Embryonic development within the cattle is similar to that of the mouse, but occurs over a much longer gestation period of approximately 285 days, although this can vary significantly depending on breed as well as environmental factors (Andersen & Plum, 1965). According to

Waters (2013) during bovine embryogenesis the embryo divides to 2 cells on E1.0, 4 cells by E1.5 and consists of 8 cells by the end of E3.0. The morula forms on E5.0 at the 16-32 cell stage and travels down the oviduct entering the uterus between E5.0 and E6.0. The morula is then compacted during E6.0 initiating the formation of the blastocoel cavity, with blastocyst development beginning on E7.0 (Lindner & Wright, 1983). On E8.0 there is continued expansion of the blastocyst and the ICM is formed, with the blastocyst hatching from the zona pellucida on E9.0 (Chang, 1952). Between E15 and E17 there is maternal recognition of pregnancy and at E18 portions of the developing cells become the placenta along with formation of the primitive groove and emergence of the notochord (Greenstein & Foley, 1957). Implantation occurs by E19 with adhesion being complete by E22, (King, Atkinson, & Robertson, 1980). According to Maddox (2003) primitive streak and neural groove formation occurs on E21. By E23 the bovine embryo has complete formation of the hypoblast and epiblast, establishment of the amniotic cavity, formation of the primitive streak (with precursor cells previously formed at E14), endoderm and mesoderm formation, and neurulation and differentiation of mesodermal cells. Limb development begins on E25 as well as organogenesis (Waters, 2013). Fourie (1990) recognizes the critical stage of limb development within the bovine fetus is from Day 24 to 40 of gestation. Like that of the mouse, the majority of bovine fetal growth occurs during the last trimester of gestation until birth where 75% of its total fetal weight is gained (Waters, 2013).

1.5 Gene-editing

Genome editing is the process of editing an organism's DNA by removal, addition or alteration of nucleotides to its genome (Kim 2015). Current genome editing methods have the capability to alter virtually any gene in a diverse range of cell types and organisms (Gaj,

Gersbach, & Barbas, 2013). The first report of direct introduction of new genetic material into an embryo came from Jaenisch and Mintz (1974) with the discovery that viral DNA sequences could be detected in somatic tissues after SV40 DNA, a virus with the potential to cause tumor growth, was injected into the blastocoele cavity of mouse blastocysts (Jaenisch & Mintz, 1974).

A whole new era of genome editing began after Gordon's (1980) discovery that exogenous DNA can be efficiently incorporated into a mammal's chromosomes when injected into the nucleus. This incorporation of new DNA occurs through homologous recombination in which DNA molecules recombine with each other through their shared homologous regions. Bradley and Evans et al. (1984) successfully completed blastocysts injection techniques to provide evidence of embryonic stem cells (ES) contribution to functional germ cells. They then went on to discover ES cells could be used to introduce genetic material into the germline. Their experiment consisted of infecting ES cells with a recombinant retrovirus before injection into blastocysts. The study was successful after confirmation of the retroviral DNA in the founders and F1 offspring (Evans, Bradley, Kuehn, & Robertson, 1985). Morgan and Capecchi (1986) successfully used this technique to correct a defective gene by injecting copies of the same gene with a different mutation into the mammalian nucleus. After first establishing cell lines with a mutant gene integrated into the host's genome, Morgan and Capecchi injected DNA containing a different mutation within the gene, resulting in the restoration of the gene through homologous recombination.

The discovery that targeted DNA double stranded breaks (DSBs) could be used to stimulate endogenous cellular repair machinery set the foundation for gene-editing (Takata et al., 1998). DSBs occur from events such as ionizing radiation, spontaneous DNA replication, and by programmed endonucleases that cleave the phosphodiester bond (Haber, 2000). Mao (2008)

states that both strands of the double helix are broken during a DSB and can ultimately lead to genome rearrangement. Specifically, if a DSB is left unrepaired, or repairs itself in the wrong way, it could result in the loss of genetic information or genetic rearrangements. These events can lead to a loss of gene function affecting key pathways. For example, if enough damage is done by an unrepaired DSB, an apoptotic gene pathway could be activated at the wrong time during development, resulting in excess cell death (Mao, et al., 2008). Within eukaryotes, there are two known general DSB repair pathways, homologous recombination (HR) and non-homologous end joining (NHEJ) (Takata, et al., 1998). While both pathways play important roles in the DSB repair process, HR results in more accurate repairs while NHEJ is error prone (Gaj, et al., 2013; Maeder & Gersbach, 2016). The HR repair mechanism is cell cycle dependent, acting in coordination with the S and G2 cell cycle phases, after DNA replication but before cell division occurs and involves the use of nearby sister chromatids (Brandsma & Gent, 2012; Sonoda, Hochegger, Saberi, Taniguchi, & Takeda, 2006). HR uses regions of homology between exposed ends of the DSB and a donor DNA molecule as a template during repair (San Filippo, Sung, & Klein, 2008). In contrast, the NHEJ repair pathway is independent of homology and acts in a non-template manner, rejoining what is left of the two DNA ends producing junctions that vary in sequence (Lieber, 2008; Mao, et al., 2008).

Recent advances in genome manipulation have been made through engineered nucleases with programmable, site specific DNA-binding domains (Perez-Pinera, Ousterout, & Gersbach, 2012). There are currently several types of engineered nucleases that induce site-specific double stranded breaks; zinc finger nucleases (ZFNs) and transcription activator-like effector nucleases (TALENs) The first engineered nuclease technology, zinc finger, was first used in 2002 on *Drosophila* and mammalian cells (Ma & Liu, 2015; Pavletich & Pabo, 1991). ZFNs are highly

specific, with each domain engineered to recognize a nucleotide triplet within the genome. They are manufactured from zinc fingers, or proteins that recognize and bind to specific triplet sequences, their folding structure determined by a zinc ion. ZFNs are usually composed of 4-6 zinc finger domains fused to the non-specific nuclease domain of the FokI restriction endonuclease (Wright, Li, Yang, & Spalding, 2014) The FokI nuclease functions as a dimer, requiring two ZFNs to bind on opposite strands of the DNA in order to induce a DSB (Maeder & Gersbach, 2016). ZFN-induced DSBs are used to modify the genome by insertion or deletion through NHEJ (Ma & Liu, 2015).

The genome targeting capabilities of transcription activator-like (TAL) effectors was discovered in 2009, stimulating the engineering of a new gene editing tool known as TALENs (Moscou & Bogdanove, 2009). TALENs soon became preferred over ZFNs due to the specificity of their TALEs consisting of 33-35 amino acid repeat domains, each domain recognizing a single base pair (Ma & Liu, 2015). The specificity of base recognition is determined by the hypervariable amino acids 12 and 13 that interact with the targeted DNA bases, also known as repeat-variable di-residues (RVDs) (Boch et al., 2009). There are four major RVDs; HD, NI, NG and NN that most commonly bind to cytosine, adenine, thymine, and guanine respectively (Wright, et al., 2014). TALE repeats are then linked together to recognize continuous DNA sequences. Like ZFN, these TALEs are fused with the sequence independent FokI endonuclease at the c-terminal end of the protein inducing the DSB. Their targeting range, simple DNA code and ease of engineering has led to their popularity as artificial transcription factors and nucleases; as of 2014, TALENs have been successfully used in over 25 species including plants, zebra fish, frogs, rats, pigs, mice, and in human somatic and pluripotent stem cells.

The latest gene-editing technology, clustered regularly-interspaced short palindromic repeat (CRISPR)/CRISPR-associated (Cas) systems, (CRISPR/Cas9), has the ability to target many genes at once, providing an advantage for studying complex diseases caused by many genes acting together. There are currently three types of CRISPR systems (I, II, III) with type II being the most common due to its single protein requirement, Cas9, for target cleavage (Pruett-Miller, 2015). Cas9 is a RNA-guided nuclease that is able to bind to target DNA and induce a DSB (Garneau et al., 2010). According to Ran (2013), CRIPSR/Cas is an adaptive immune system consisting of Cas genes, noncoding RNAs and a distinct array of repetitive elements. These repeats contain a variable 20 bp sequence from exogenous DNA targets or protospacers, making up the CRISPR RNA (crRNA) array. Within the target DNA, each protospacer is associated to its adjacent motif (PAM). Each crRNA contains a 20 nucleotide sequence that directs Cas9 to the targeted DNA where it induces a DSB.

Through the use of gene editing technology, model organisms carrying disease mutations are created in order to further study gene function and pathogenesis, as well as having the possibility to correct causative mutations in gene therapy. Specifically, ZFNs have been used to correct the mutations that cause the X-linked severe combined immune deficiency (SCID) (Urnov et al., 2005). Modeling gene rearrangements through TALEN technology has led to the discovery of a drug resistant mechanism in prostate cancer (Wright, Li et al. 2014). The CRISPR/Cas9 system has been successfully used to correct disease-related genes in the mouse and in intestinal stem cells of a cystic fibrosis patient (Wu et al., 2013). Overall, these tools are revolutionizing biological research and medicine with the improving ability to understand and treat disease.

Chapter 2: Characterization of a Mouse Model for Bovine Developmental Duplications

2.1 Introduction

Developmental Duplications is an autosomal recessive genetic condition recently discovered in Angus cattle. It is a congenital abnormality where duplication of the neural crest derived tissues occurs during embryonic development. Congenital limb abnormalities are relatively common in domestic animals and humans (Fourie, 1990). However, while sporadic cases in cattle have been reported in both *Bos taurus* and *Bos indicus* breeds around the world, Denholm (2011) reported that polymelia seemed to be rising above the sporadic level in Australia among registered Angus cattle. At least fifteen cases were reported in newborn Angus calves within two years, with many other cases being reported in the US. This observation suggested the possibility of an emerging heritable defect. The majority of bovine cases are noted as notomelic, with the extra forelimbs being attached along the dorsal midline. A common phenotypic presentation of the condition includes calves born with various forms of polymelia (notomelia, cephalomelia, pygomelia), having frequent duplication of the front limbs originating from the neck or shoulder region. Calves homozygous for this mutation also show congenital malformations associated with neural tube defects. Malformations include myelomeningocele, split cord malformation, spinal embryonic teratoma, sacral and occipital myolipoma, encephalocele, and craniofacial dysmorphogenesis.

Genome wide association studies identified a single locus associated with the DD phenotype. Further investigation identified a nonsynonymous valine to alanine substitution in exon 5 of the NHLRC2 gene, a locus where valine is invariable in 53 known species of diverse taxa (Figure 2). Penetrance of DD phenotypes of affected individuals is less than 50% (L. J. Denholm, et al., 2016). Due to its incomplete penetrance and undetected embryonic loss,

population allele frequency was ~3% in the United States and ~7% in Australia by the time DD was recognized as a syndrome. The purpose of this study was to confirm the role of *NHLRC2* in DD and to further characterize the role *NHLRC2* in mammalian development through use of a mouse model.

2.2 Materials and Methods

TALEN Generated Mice

NHLRC2 gene-edited mice were produced in the Friend Virus B (FVB) mouse strain using TALENs (Cyagen Biosciences, Inc.). TALs and TALEN vectors were assembled by Cyagen Biosciences using the Golden Gate method (Cermak, et al., 2011). TALEN mRNA was generated by *in vitro* transcription and injected into fertilized eggs for gene-editing. FVB mice are ideal for transgenic or knockout model development due to their prominent pronuclei in fertilized eggs along with their large litter size (The Jackson Laboratory).

Upon delivery from Cyagen Biosciences, mice were subjected to a quarantine protocol in the Division of Animal Resources Rodent Quarantine Facility. The quarantine protocol included disease testing of mice along with sentinel animal exposure and testing. Imported mice were checked for parasites and had blood drawn for initial serology testing. After 7 weeks, sentinels were euthanized for serology and parasitology testing. No agents of concern were identified and gene-edited mice were released from quarantine after nine weeks. Mice were kept in a 12-hour light/12-hour dark regimen with Standard Mouse Chow and water available at all times. Mice were initially housed separately. Litters born at the University of Illinois at Urbana-Champaign Rodent Facility were then housed together based on gender and genotype.

Animal Husbandry

A total of 15 founder mice were received. Founder mice were heterozygous for one of three NHLRC2 mutations induced by TALEN-editing. The heterozygous founder mice within each line were initially mated to wild type (WT) FVB mice to increase the size of the breeding population. The resulting heterozygous offspring were then intermated to phenotypically characterize homozygous progeny. Mice were assumed to be sexually mature and optimal for breeding at six weeks of age (Lambert, 2007). Breeding was performed by placing one male with two to four females per cage for a one week period. Following the mating period, pregnant females were caged separately to allow for examination of the genotype ratio in each litter for each female. Additionally, individual housing of females was used to prevent excess cannibalism of dead pups.

Evidence of copulation was used as a method to harvest embryos of known gestational age. Before 10 A.M. on the morning following the initial exposure of females to a male, each female was examined for the presence of a vaginal plug (Silver & Barsh, 1995). Once a plug was detected, the female was removed from the cage and assumed to be pregnant. At a predetermined gestational age, females were euthanized and reproductive tracts were harvested as described below (see Dissection).

PCR Genotyping

Oligonucleotide primers for genotyping were designed using Primer Designer v2.0 (Scientific and Educational Software). Primers were designed to flank the targeted mutation site in exon 5 of mouse NHLRC2. PCR amplification of the wild-type allele using the primers NHLDNAF 5’-AGCCAGCCTTCTATGACACT-3’ and NHLDNAR 5’-

TCCCTTGAATACCGACACCA-3' was predicted to produce a 167 bp amplicon. The reverse primer was fluorescently labeled with 6-FAM for fragment detection using an automated DNA sequencing instrument.

Ear notching was used for individual mouse identification and simultaneous collection of tissue samples for DNA isolation. Genomic DNA was isolated using the Quick-gDNA™ MiniPrep kit according to the manufacturer's recommendations (Zymo Research, Irvine, CA). Following extraction, genomic DNA was quantified by spectrophotometry using a NanoDrop instrument (Thermo Fisher Scientific, Inc.).

PCR amplification was performed in 10 μL reactions with each reaction composed of 1X Qiagen PCR buffer, 0.1 μM each primer, 200 μM each dNTP, and 0.025 U/μL Qiagen HotStarTaq DNA polymerase. Thermal cycling parameters include 5 minutes of initial activation at 95°C followed by 30 cycles of 30s at 94°C, 30s at 56°C and 30s at 72°C; this was followed by 15 minutes at 72°C and 5 min at 10°C. To verify PCR quality, 5 μL of each reaction were mixed with 2 μL of 6X loading dye (15% Ficoll, 0.01% bromophenol blue) and subjected to electrophoresis in a 2% 0.5X TBE agarose gel containing 100 ng/mL ethidium bromide. Following electrophoresis DNA fragments were visualized under UV illumination.

Three μL of each PCR product was diluted with 80 μL of Optima water. Subsequently, 3 μL of diluted PCR product were then dried in a vacuum evaporator. Dried samples were sent to W.M. Keck Center for Comparative and Functional Genomics at the University of Illinois for fragment analysis. The GeneScan™ 600 LIZ® size standard (Thermo Fisher) was used for assignment of fragment sizes. Genotypes were analyzed using GeneMarker™ V1.91 software (Softgenetics, State College, PA, USA).

Sequencing

Forward and reverse primers for cDNA amplification were designed using Primer Designer v2.0 (Scientific and Educational Software) beginning at exon 3 and ending at exon 6, flanking known deletions in exon 5. Product size of cDNA amplification was 438 bp.

Total RNA was extracted from whole brains of three heterozygous mice for each of the three mutations. Extraction was performed using TRIzol® reagent (Invitrogen™, Life Technologies Corporation) according to the manufacturer's recommendations. Total RNA was quantified by spectrophotometry using a Nanodrop instrument (Thermo Fisher Scientific, Inc.). Quality of the RNA was assessed by electrophoresis in a 1.2% formaldehyde-1X MOPS agarose gel. Formaldehyde gel loading buffer was added to samples before loading. Prior to cDNA synthesis, 10 μg of total RNA was repurified using the RNeasy Mini Kit as described by the manufacturer (Qiagen).

Complementary DNA (cDNA) was synthesized in a 20 μL reaction by first combining 2 μg RNA, 0.5 μM random decamers, and 0.5 mM dNTPs in a total volume of 13 μL followed by incubation at 65°C for 5 minutes and then snap cooled on ice for at least one minute. After cooling, reagents were added for a final concentration of 1X First strand cDNA synthesis buffer, 5 μM DTT, 2 Units/μL RNaseOUT Recombinant RNase Inhibitor, and 10 Units/μL Superscript III reverse transcriptase. The resulting mixture was incubated at 25°C for 5 minutes for annealing random decamers, and then at 50°C for one hour. Reactions were inactivated by incubation at 70°C for 15 minutes. Optima™ water (Fisher Scientific) was added to dilute the total volume to approximately 100 μL. PCR amplification was performed in 20 μL reactions with each reaction composed of 1X Qiagen PCR buffer, 0.5 μM each primer, 200 μM each dNTP, and 0.025 U/μL Qiagen HotStarTaq DNA polymerase. Thermal cycling parameters include 5 minutes of initial

activation at 95°C followed by 30 cycles of 30s at 94°C, 30s at 54°C and 30s at 72°C; this was followed by 15 minutes at 72°C and 5 minutes at 10°C. To verify product quality, amplicons were separated via electrophoresis on a 2% 0.5x TBE agarose gel containing 100 ng/μL ethidium bromide. A 2-log DNA ladder was used as a size reference (New England BioLabs).

Cloning of PCR amplicons was performed using the NEB PCR Cloning Kit according to the manufacturer's protocol. A 10 μL ligation reaction was prepared by first combining 1 μL of linearized pMiniT™ Vector with 1-2 μL of PCR product and adding Optima™ water up to 5 μL total volume. Then, cloning master mix was added to a final concentration of 1X and the ligation mixture was incubated at room temperature (25°C) for 5 minutes and then on ice for 2 minutes. Reactions were then transformed immediately into NEB 10-beat competent *E. coli.* Competent cells were first thawed on ice for 10 minutes before transformation. Two μL of each ligation reaction were added to cells for a 25:1 ratio and mixed by flicking of the tube five times. The mixture was incubated on ice for 30 minutes, heat shocked at 42°C for 30 seconds and then put back on ice for 5 minutes. SOC media was added for a total volume of approximately 1 mL. Cultures were placed at 37°C for 60 minute with agitation at 250 rpm for cell recovery. Cells were then mixed thoroughly by inversion and 50 μL of the cultures were spread onto 37°C pre-warmed agar plates containing 100 μg/ml ampicillin. Plates were inverted and incubated at 37°C overnight.

Eight colonies from each plate were picked using sterile toothpicks and separately grown in 3mL of 2X Luria-Berani (LB) medium in snap cap tubes. Cultures were incubated with shaking overnight (18 hours) at 37°C. Plasmid DNA was purified using the the QIAprep Spin Miniprep Kit (Qiagen) according to the manufacturer's recommendations. Plasmids were digested with *Eco* RI (New England Biolabs) to confirm presence of inserts. Total reaction

volume was 10 μL, consisting of 1 μL plasmid DNA, 1X NEB buffer 4, and 6 Units of EcoRI. Digestion reactions were incubated at 37°C for 1 hour and were analyzed by electrophoresis in a 1.2% 0.5X TBE agarose gel containing 100 ng/mL ethidium bromide. Following electrophoresis DNA fragments were visualized under UV illumination.

After confirming that plasmids contained inserts, sequencing was performed in an 8.0 μL reaction volume containing 3.62 μL Sanger sequencing buffer (.16 M Tris pH 9.0, 3 mM $MgCl_2$, 4.9% tetramethylene sulfone and 0.001% tween 20), 0.25 μL BigDye® (Applied Biosystems), 0.08 μL BigDye® dGTP (Applied Biosystems), and 1.31 μM NEB forward or reverse primer, with 1 μL of plasmid DNA. Thermocycling parameters include 90 seconds of initial activation at 96°C, followed by 54 cycles of 15s at 96°C, 15s at 53°C, and 3 minutes at 60°C; this was followed by 10 minutes at 60°C with a 10°C hold. Sequencing products were purified using a size exclusion with Sephadex G50. Sephadex was first rehydrated with 300 μL Optima water in a 25-30 MBPP Whatman® Unifilter® 96-well plate and put in fridge overnight. The plate was centrifuged at 750g for 2 minutes to remove excess water. Sequencing reactions were added to the Sephadex matrix and the plate was centrifuged for 2 minutes at 750g and eluent was collected in a nonskirted 96-well plate. Samples were then submitted to the W.M. Keck Center for Comparative and Functional Genomics for analysis. Sequence data was gathered using an ABI 3730XL DNA Analyzer (Applied Biosystems). Data was analyzed using CodonCode Aligner software.

Embryo Collection

Female mice were euthanized by CO_2 inhalation followed by cervical dislocation. The euthanized female was placed supine and the abdomen was sterilized with 70% ethanol to reduce

the risk of contamination from maternal hair. The abdominal skin was pinched and a small lateral incision was made at the midline with regular surgical scissors. The skin was then pulled apart toward the head and tail, exposing the abdomen. The peritoneum was then cut to expose the abdominal cavity. Intestines and excess fat obscuring sight of the uterus was pushed aside to reveal reproductive organs. The uterine horns were removed by grasping the uterus below the oviduct and cutting it free along the mesometrium. Dissected uteri were placed in Dulbecco's phosphate-buffered saline solution (PBS) in a petri dish and placed under a dissecting microscope (Shea & Geijsen, 2007). Fatty tissue was first cut away from the uterus. Each embryo proper is surrounded by visceral yolk sac, parietal yolk sac and the decidua, appearing as "beads on a string" along the uterus (Udan & Dickinson, 2010). Yolk sacs (or "beads") were separated by carefully cutting in between implantation sites (in between beads) and were each placed in separate petri dishes containing PBS to avoid further contamination. The muscle layer of each sac was peeled back to expose the decidua. The distal region of the decidua is more pointed than the wider ectoplacental cone at the proximal region (Udan & Dickinson, 2010). The apex portion of the decidua was clipped to expose the midventral or distal tip of the enclosed embryo. The embryo was then dissected out after carefully tearing decidua apart. Removal of residual Reichart's membrane and ectoplacental cone was carefully performed to ensure detachment of all maternal components that could interfere with genotyping. Instruments were washed in PBS between embryos. Embryos were placed in 1.7 ml microcentrifuge tubes for subsequent DNA extraction and genotyping analysis as previously described.

Hormone injection

Female mice of each line were superovulated for embryo flushing according to Hogan et al.'s (1994) manual on Manipulating the Mouse Embryo. Female mice were picked up by the scruff of the neck, ensuring the head was held in place to prevent being bitten. The tail was twisted around the little finger to ensure no other movement occurred. Ten IU of equine chorionic gonadotropin (eCG) was injected intra-peritoneally, taking care to avoid the diaphragm and bladder, waiting briefly before needle withdrawal to ensure solution was injected correctly. Ten IU of human chorionic gonadotropin (hCG) was then injected intraperitoneally prior to the release of endogenous luteinizing hormone and 48 hours after eCG to induce ovulation. Following the hCG injection, a single female was placed with a single male overnight as described above. Females were observed for vaginal plugs the next morning, indicating day E0.5. If no plug was observed, females were still euthanized on the desired day in order to account for potential mating. On E3.5, females were euthanized, their reproductive organs were dissected as previously described and placed in a petri dish containing 2% fetal bovine serum (FBS) in PBS. Flushing of day E3.5 blastocysts was executed according to Hogan et al.'s manual on Manipulating the Mouse Embryo and performed by Dr. Marcello Rubessa (UIUC, Animal Sciences, Laboratory of Reproductive Biology and Tissue Engineering). Flushed blastocysts were placed in a 96-well plate for whole genome amplification using the Repli-g Mini Kit (Qiagen) according to manufacturer's recommendations.

Statistical Methods

Pairwise t-tests for comparing litter sizes were performed. Chi-square goodness-of-fit was used to test deviation from Mendelian inheritance ratios. A significance threshold of $p<0.05$ was used.

2.3 Results and Discussion

In cattle, a mutation in NHLRC2 that results in the non-synonymous substitution of a highly conserved amino acid residue, p.V311A, is associated with numerous congenital abnormalities. Many of these abnormalities are similar to NTDs known to be associated with the disruption of neurulation. To further investigate the role of *NHLRC2* in development, the NHLRC2 locus in mice was targeted for gene-editing. TALENs were designed to target the 5' end of exon 5 in the mouse NHLRC2 gene. TALEN target sites flanked the orthologous region '

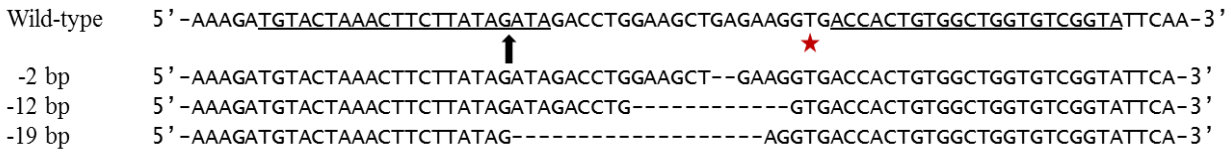

Figure 2.1. Comparison of NHLRC2 allelic DNA sequences between wild-type and TALEN-edited mouse lines. The underlined sequences correspond to the TALEN target sites. The black arrow indicates the 5' splice junction for exon 5 of mouse NHLRC2. The red star shows the orthologous nucleotide position of the mutation associated with DD in cattle.

of the known bovine mutation in an effort to model the cattle disease as closely as possible (Figure 2.1).

Cyagen Biosciences, Inc. was contracted to perform the gene-editing in the FVB mouse strain by nuclear injection of TALEN mRNAs into mouse zygotes. Three mice were identified following the initial mutation screening (Table A.1). These founder mice were used to generate

F1 animals to establish individual breeding lines (Table A.1). Gene-editing was confirmed by sequencing NHLRC2 in the founder individuals. Comparison between these sequences and the wild-type NHLRC2 sequence showed that all three mutations were deletions within the targeted region (Figure 2.1). Deletions of -2 bp, -12 bp, and -19 bp were detected (Figure 2.1). However, none of the gene-editing events resulted in the modification or deletion of the codon that is mutated in cattle (Figure 2.1)

Due to the proximity of the deletions to the 5' splice junction of exon 5 (Figure 2.1), these mutations had an increased probability of altering normal splicing pattern within NHLRC2, potentially affecting the protein coding functions and functional properties of NHLRC2 (Ward and Cooper 2010). Thus, sequencing of the cDNA for each allele was conducted to confirm each mutation's impact on the encoded NHLRC2 protein. In mice, *NHLRC2* is highly expressed within the brain, making this tissue ideal for RNA extraction and subsequent cDNA synthesis. Whole brains were isolated from a heterozygous mouse corresponding to each mutation and total RNA was isolated. Sequence analyses showed no changes in splicing due to these deletions

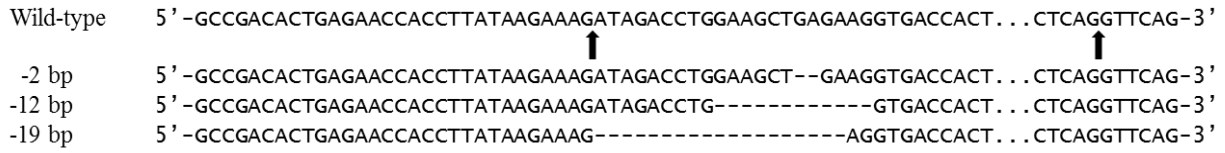

Figure 2.2. Comparison of NHLRC2 cDNA sequences between wild-type and TALEN-edited mouse lines. The black arrows indicate the splice junctions between exons 4 and 5 (left arrow), and exons 5 and 6 (right arrow) of mouse NHLRC2.

(Figure 2.2). All sequences generated showed the predicted cDNA sequence based on the location of the introduced mutations (Figure 2.2). One sequence indicated that exon 4 of mouse NHLRC2 may be alternatively spliced (data not shown).

Translation of the cDNA sequences for each of the gene-edited alleles shows that two of the mutations, -2 bp and -19 bp, produce frameshift mutations as would be expected based on the number of nucleotides deleted. Although both of these mutations are likely to produce transcripts that would be degraded due to nonsense-mediated RNA decay (Hentze & Kulozik, 1999), truncation of translation is significantly different for these transcripts (Figure 2.3). For the -2 bp mutation, translation of the corresponding mRNA is predicted to extend 43 amino acids beyond the mutation (data not shown). In comparison, the -19 bp allele results in the introduction of a stop codon in the second codon of the modified exon 5 sequence (Figure 2.3). However, both transcripts would encode proteins less than half the normal length of NHLRC2 if translated. In contrast to these frameshift mutations, the -12 bp deletion is predicted to produce a protein that is missing the four amino acid residues immediately upstream of the substitution associated with DD in cattle (Figure 2.3).

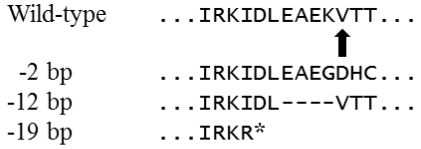

Figure 2.3. Alignment of translated protein sequences for the wild-type and TALEN-edited alleles. The arrow indicates the highly conserved valine residue at position 311 of the NHLRC2 protein that is substituted with an alanine residue in DD. Dashes represent the four deleted amino acid residues as a result of the 12 bp deletion following gene-editing. The asterisk indicates a premature stop codon introduced as a result of the frameshift in the -19 bp allele.

A genotyping assay was successfully developed to facilitate the efficient and accurate genotyping of mice produced from experimental matings that were performed to characterize the phenotypic effects of these NHLRC2 mutations in each of the three mouse lines. Due to the small size of these deletions and the presence of multiple alleles, a genotyping assay based on

size differentiation of PCR-amplified fragments was developed (Figure 2.4). PCR primers were designed flanking the identified deletion mutations. Detection of PCR amplicons was facilitated by the labeling of one primer with the fluorescent dye 6-FAM. The performance of the assay was generally robust with no ambiguity in genotype assignment (Figure 2.4).

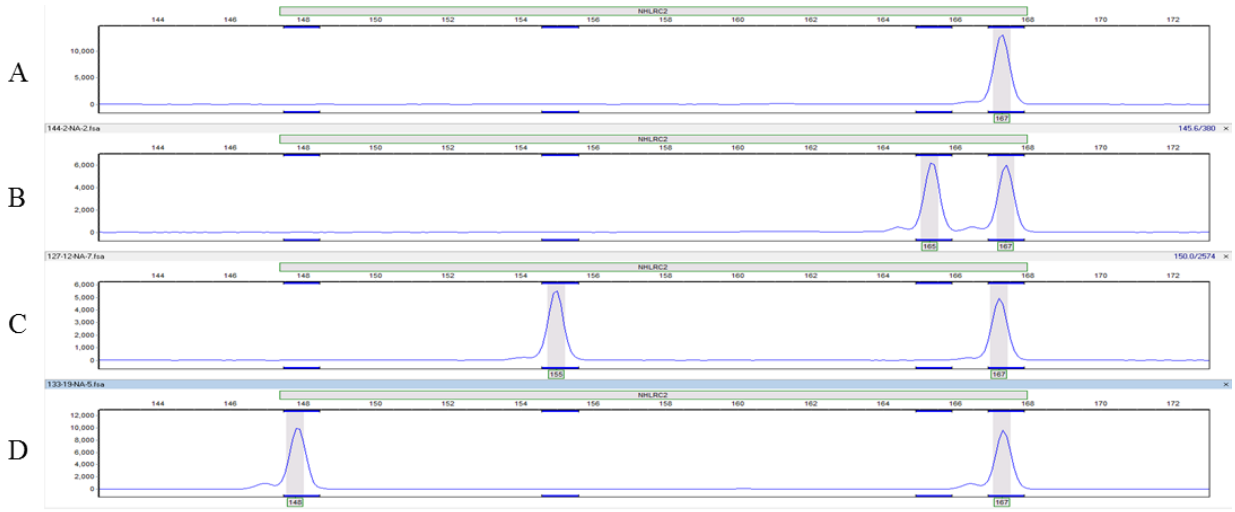

Figure 2.4. Digital electrophoretograms showing the fragments generated from the PCR-based genotyping assay for mouse NHLRC2. Each panel (A-D) corresponds to a single individual. Fluorescently labeled fragments are shown as peaks on the electrophoretogram. The relative size of each fragment is demonstrated by the position of the peak along the X-axis. Fragment sizes increase moving from left to right along the axis. Panel A represents a homozygous wild-type mouse showing only the 167 bp allele. Panels B-D represent mice heterozygous for each of the TALEN-generated deletion mutations of -2 bp, -12 bp, and -19 bp, respectively. The wild-type allele, with a fragment size of 167 bp, is present in all three heterozygous individuals as well as fragments of 165 bp, 155 bp, and 148 bp, corresponding to each of the deletion alleles, respectively.

Initially, matings between wild-type (WT) FVB mice and NHLRC2-edited F1 mice were performed to expand the population size. Matings between WT and F1 mice demonstrated that progeny heterozygous for each mutation appear phenotypically normal. This was expected based on the F1 mice received from Cyagen Biosciences, as well as the recessive inheritance pattern of

DD in cattle. Thirty-one matings between WT and heterozygous mice yielded a total of 267 offspring. Within each genetic line, average litter size and segregation ratio was examined to confirm there was no impact of these mutations in a larger breeding population. Average litter size within each line ranged from 8.0 to 9.3 pups per litter (Table 2.1). After performing two sample T-tests assuming equal variance, there was no statistical differences in litter size detected between lines ($p>0.05$; Table A.3). Although no matings between WT mice were done, the overall average litter size in this population appears similar to that reported in the literature for the FVB strain of 9.5 pups/litter (Silver & Barsh, 1995).

Table 2.1. Average Litter Size of WT x Heterozygous Matings

Mating Type	No. of Litters	Average Litter Size
WT x -2 bp	8	9.3
WT x -12 bp	13	8
WT x -19 bp	10	8.9

Segregation of alleles for each line in WT x heterozygote matings also appears consistent with the expected Mendelian 1:1 inheritance pattern (Table 2.2). There were no indications that heterozygosity for these mutations has any impact on survivability as evidenced by relatively small deviations from the expected ratios (Table 2.2; Tables A.4).

Table 2.2. Summary Chi-square Statistics for Allele Segregation in WT x Heterozygote Matings

	Genotype			
Mating	WT	Heterozygous	X^2	P Value
WT x -2 bp	39	35	0.22	0.64
WT x -12 bp	55	49	0.35	0.55
WT x -19 bp	43	46	0.10	0.75

Heterozygous matings from each line were conducted to observe phenotypic effects associated with these mutations for comparison to those seen in cattle with DD. A total of 52 matings between heterozygous mice yielded 328 offspring. In contrast to the WT x heterozygous matings, the litter sizes observed for these matings was significantly smaller with an overall average litter size of 6.4 pups versus 8.6 pups (Table 2.3). Comparison of litter sizes between lines using two sample T-tests assuming equal variances indicated that the -2 bp line had an average litter size that was significantly smaller than the -19 bp line ($p<0.05$; Table A.3) with a trend toward being significantly smaller than the -12 bp line ($p<0.10$; Table A.3). There was no difference in litter size between the -12 bp and -19 bp lines.

Table 2.3. Average Litter Size of Heterozygous x Heterozygous Matings

Mating Type	No. of Litters	Average Litter Size
-2 bp x -2 bp	17	5.2
-12 bp x -12 bp	17	6.7
-19 bp x -19 bp	12	7.5

The underlying basis of the significantly smaller litter sizes was revealed following the genotyping of offspring from heterozygous matings. For all three NHLRC2 gene-edited lines, no offspring were genotyped as homozygous for any of the introduced mutations (Table 2.4). Goodness-of-fit analyses clearly demonstrates that offspring genotype ratios from these matings are not consistent with the expected Mendelian segregation ($p<0.0001$; Table 2.4). As confirmation, progeny ratios were tested under a model of lethal inheritance and found not to deviate from expected ($p>0.05$; Table A.4).

Table 2.4. Summary Chi-square Statistics for Allele Segregation in Heterozygote x Heterozygote Matings

	Genotype				
Mating	WT	Heterozygous	Homozygous Recessive	X^2	P Value
-2 bp x -2 bp	23	65	0	32.07	<0.001
-12 bp x -12 bp	41	73	0	38.47	<0.001
-12 bp x -12 bp (E8.5)	10	15	0	9.00	0.011
-19 bp x -19 bp	31	59	0	30.07	<0.001

The clear absence of homozygous recessive offspring along with decreased litter size demonstrated that these mutations were embryonically lethal in mice. Even so, additional matings were conducted to characterize the developmental time point where embryonic death was occurring. Phenotypes of cattle affected with DD consist of NTD lesions and neural crest derived tissue duplications. It is hypothesized that these are the result of improper neural tube closure. Thus, the developmental time point of the initiation of neural tube closure in the mouse embryo was investigated (E8.5) (J. Gray & Ross, 2011). Five female mice from heterozygous -12 bp matings with successful plug detection were dissected at E8.5, their embryos were

extracted for genotyping. The -12 bp line was chosen due to the potential of this mutation, with its deletion of four complete amino acids, having a higher survival rate. Yolk sacs containing no embryos were observed with each dissection. The number of yolk sacs exceeded the number of live births by 68.7% (11.3 vs. 6.7). The five dissections yielded 26 embryos consisting of 10 WT and 15 heterozygous genotypes. The absence of homozygous recessive genotypes indicated that embryonic death was occurring between fertilization and E8.5. However, the number of yolk sacs from these E8.5 dissections exceeded the number of live births with this mutation by 68.7% (11.3 vs 6.7). This gives indication implantation had occurred but further development of the embryo did not occur (Flores, Hildebrandt, Kühl, & Drews, 2014). Images of seven E8.5 extracted embryos from a heterozygous -12 mating were captured on a Nikon stereoscopic zoom microscope and subsequently genotyped. Genotyping analysis revealed two heterozygotes and five WT embryos. No physical differences between heterozygous and WT E8.5 embryos were observed (Figure 2.5).

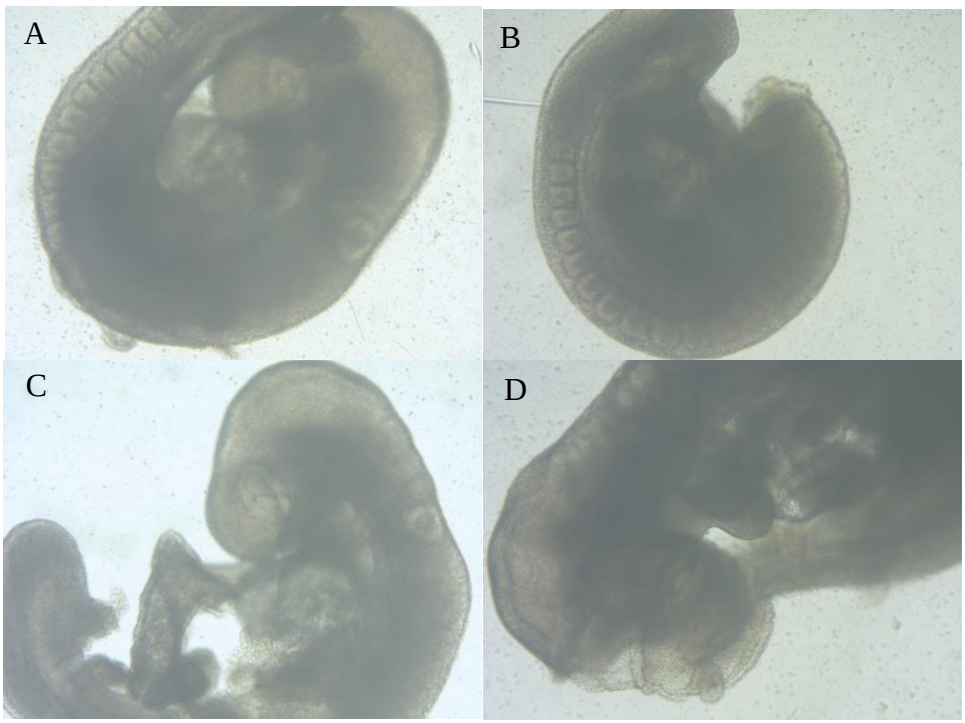

Figure 2.5. Comparison of microscopic images of E8.5 embryos from a -12 bp heterozygous mating after the initiation of neural tube closure. Panel A represents a heterozygous embryo. Panel B-D represent WT embryos.

Embryo flushing was performed at E3.5 when an embryo becomes a blastocyst, but approximately 24 hours prior to implantation (Fong, et al., 1998). Seven embryos from a -12 heterozygous mating were obtained. Whole genome amplification of blastocysts followed by genotyping by fragment analysis resulted in all heterozygotes. The absence of homozygous recessive blastocysts would lead us to theorize that death occurred before implantation, however the absence of WT genotypes leads us to conclude that there was occurrence of contamination by maternal cells that may have been amplified when performing whole genome amplification.

From the discovery that mutations within *NHLRC1*¸ a family member of *NHLRC2*, plays a role in neurodegeneration within Lafora disease, leads us to believe that mutation within

NHLRC2 also effects the p53 mediated cell death pathway, leading to an increase in proapoptosis (Upadhyay, et al., 2015). Apoptosis, or programmed cell death, plays an important role in overall mammalian development, also playing a key role during central nervous system development, occurring mainly during the bending and fusion of the neural folds, neural tube remodeling and migration of neural crest cells (De Zio, Giunta, Corvaro, Ferraro, & Cecconi, 2005; Massa, et al., 2009). Proapoptosis, or excessive cell death, would result in an insufficient amount of cells needed to complete neurulation, specifically neural tube closure, resulting in NTDs. A lack of apoptosis has also been shown to be correlated with NTDS, showing the importance of the required amount of neurulation and successful neurulation (Massa, et al., 2009). DD affected calves with polymelia have extra limbs from the CNS region, suggesting that extra limbs were derived from neural crest cells that may have escaped during proapoptotic events during neurulation. Affected individuals also display lesions from NTDs, also leading us to theorize there is proapoptotic factors during neurulation that contribute to the development of lesions.

2.4 Conclusion

We have examined the role of NHLRC2 has in mammalian development by generating a mouse model deficient in this gene with varying affects. Heterozygous mice appeared phenotypically normal and the absence of homozygous recessive offspring suggests embryonic lethality. Dissection of E8.5 embryos and the observance of empty yolk sacs suggests death occurs after implantation but before the initiation the closure of the neural tube. It is suggested that like its family member *NHLRC1*, mutations in *NHLRC2* results in proapoptotic events leading to incomplete neurulation. This study showed that mutation within the *NHLRC2* gene in the mouse has more of an impact than cattle, as expected due to the subtle amino acid

substitution in bovine, but enhances the theory that this gene plays an important role in mammalian development.

References

Alberts, B., Johnson, A., Lewis, J., Raff, M., Roberts, K., & Walter, P. (2002). Cell Junctions, Cell Adhesion, and the Extracellular Matrix (4 ed.). New York: Garland Science. Retrieved from http://www.ncbi.nlm.nih.gov/books/NBK21047/.

Andersen, H., & Plum, M. (1965). Gestation Length and Birth Weight in Cattle and Buffaloes: A Review1,2. *Journal of Dairy Science, 48*(9), 1224-1235. doi: http://dx.doi.org/10.3168/jds.S0022-0302(65)88431-4

Arnér, E. S. J., & Holmgren, A. (2000). Physiological functions of thioredoxin and thioredoxin reductase. *European Journal of Biochemistry, 267*(20), 6102-6109. doi: 10.1046/j.1432-1327.2000.01701.x

Boch, J., Scholze, H., Schornack, S., Landgraf, A., Hahn, S., Kay, S., . . . Bonas, U. (2009). Breaking the Code of DNA Binding Specificity of TAL-Type III Effectors. *Science, 326*(5959), 1509-1512. doi: 10.1126/science.1178811

Botstein, D., White, R. L., Skolnick, M., & Davis, R. W. (1980). Construction of a genetic linkage map in man using restriction fragment length polymorphisms. *American Journal of Human Genetics, 32*(3), 314-331.

Brackmann, F. A., Kiefer, A., Agaimy, A., Gencik, M., & Trollmann, R. (2011). Rapidly Progressive Phenotype of Lafora Disease Associated With a Novel NHLRC1 Mutation. *Pediatric Neurology, 44*(6), 475-477. doi: http://dx.doi.org/10.1016/j.pediatrneurol.2011.01.012

Bradley, A., Evans, M., Kaufman, M. H., & Robertson, E. (1984). Formation of germ-line chimaeras from embryo-derived teratocarcinoma cell lines. [10.1038/309255a0]. *Nature, 309*(5965), 255-256.

Brandsma, I., & Gent, D. C. (2012). Pathway choice in DNA double strand break repair: observations of a balancing act. *Genome Integrity, 3,* 9-9. doi: 10.1186/2041-9414-3-9

Brown, T. A. (2002). Genomes. In O. Wiley-Liss (Ed.), Genomes (2 ed.): Oxford: Wiley-Liss. Retrieved from http://www.ncbi.nlm.nih.gov/books/NBK21116/.

Chan, E. M., Young, E. J., Ianzano, L., Munteanu, I., Zhao, X., Christopoulos, C. C., . . . Scherer, S. W. (2003). Mutations in NHLRC1 cause progressive myoclonus epilepsy. [10.1038/ng1238]. *Nat Genet, 35*(2), 125-127. doi: http://www.nature.com/ng/journal/v35/n2/suppinfo/ng1238_S1.html

Chang, M. C. (1952). Development of bovine blastocyst with a note on implantation. *The Anatomical Record, 113*(2), 143-161. doi: 10.1002/ar.1091130203

Chee Seng, K. U., Katherine, K., & Kee Seng, C. (2001). High-Throughput Single Nucleotide Polymorphisms Genotyping Technologies. Retrieved from http://dx.doi.org/10.1002/9780470015902.a0021631 doi:10.1002/9780470015902.a0021631

Chial, H. (2008). Gene mapping and disease. *Nature Education, 1*(1), 50.

Collet, J.-F., & Messens, J. (2010). Antioxidants & Redox Signaling. *13*(8), 1205-1216. doi: doi:10.1089/ars.2010.3114

Copp, A. J. (2005). Neurulation in the cranial region – normal and abnormal. *Journal of Anatomy, 207*(5), 623-635. doi: 10.1111/j.1469-7580.2005.00476.x

Copp, A. J., & Brook, F. A. (1989). Does lumbosacral spina bifida arise by failure of neural folding or by defective canalisation? *Journal of Medical Genetics, 26*(3), 160-166.

Copp, A. J., & Greene, N. D. E. (2013). Neural tube defects – disorders of neurulation and related embryonic processes. *Wiley interdisciplinary reviews. Developmental biology, 2*(2), 213-227. doi: 10.1002/wdev.71

Copp, A. J., Greene, N. D. E., & Murdoch, J. N. (2003). The Genetic Basis of Mammalian Neurulation. [10.1038/nrg1181]. *National Review Genetics, 4*(10), 784-793. doi: http://www.nature.com/nrg/journal/v4/n10/suppinfo/nrg1181_S1.html

De Zio, D., Giunta, L., Corvaro, M., Ferraro, E., & Cecconi, F. (2005). Expanding roles of programmed cell death in mammalian neurodevelopment. *Seminars in Cell & Developmental Biology, 16*(2), 281-294. doi: http://dx.doi.org/10.1016/j.semcdb.2004.12.003

Denholm, L. (2011). Polymelia (supernumerary limbs) in Angus Calves. Flock and Herd, Case note. Retrieved from http://www.flockandherd.net.au/cattle/reader/polymelia.html

Denholm, L. J., Parnell, P. F., Marron, B. M., Delhotal, J. D., Moser, D. W., & Beever, J. E. (2016). *A comparative review of Developmental Duplications (DD) in Angus cattle and neural tube defects (NTDs) in man and mouse*. Paper presented at the WBC.

Evans, M. J., Bradley, A., Kuehn, M. R., & Robertson, E. J. (1985). The Ability of EK Cells to Form Chimeras after Selection of Clones in G418 and Some Observations on the Integration of Retroviral Vector Proviral DNA into EK Cells. *Cold Spring Harbor Symposia on Quantitative Biology*, *50*, 685-689.

Flores, L. E., Hildebrandt, T. B., Kühl, A. A., & Drews, B. (2014). Early detection and staging of spontaneous embryo resorption by ultrasound biomicroscopy in murine pregnancy. *Reproductive Biology and Endocrinology : RB&E, 12*, 38-38. doi: 10.1186/1477-7827-12-38

Fly, T. I. (1996). Cubitus Interruptus.

Fong, C. Y., Bongso, A., Ng, S. C., Kumar, J., Trounson, A., & Ratnam, S. (1998). Blastocyst transfer after enzymatic treatment of the zona pellucida: improving in-vitro fertilization

and understanding implantation. *Human Reproduction, 13*(10), 2926-2932. doi: 10.1093/humrep/13.10.2926

Fourie, S. L. (1990). Congenital supernumerary ectopic limbs in a Brahman-cross calf. *61*, 68-70. Retrieved from http://www.ncbi.nlm.nih.gov/pubmed/2286989

Gaj, T., Gersbach, C. A., & Barbas, C. F. (2013). ZFN, TALEN and CRISPR/Cas-based methods for genome engineering. *Trends in biotechnology, 31*(7), 397-405. doi: 10.1016/j.tibtech.2013.04.004

Garneau, J. E., Dupuis, M.-E., Villion, M., Romero, D. A., Barrangou, R., Boyaval, P., . . . Moineau, S. (2010). The CRISPR/Cas bacterial immune system cleaves bacteriophage and plasmid DNA. [10.1038/nature09523]. *Nature, 468*(7320), 67-71. doi: http://www.nature.com/nature/journal/v468/n7320/abs/nature09523.html#supplementary-information

Gilbert, S. (2000). Formation of the Neural Tube *Developmental Biology* Retrieved from http://www.ncbi.nlm.nih.gov/books/NBK10080/

Glickman, M. H., & Ciechanover, A. (2002). The Ubiquitin-Proteasome Proteolytic Pathway: Destruction for the Sake of Construction. *Physiological Reviews, 82*(2), 373-428. doi: 10.1152/physrev.00027.2001

Gordon, J.W., Scangos, G.A., Plotkin, D.J., Barbosa, J.A., Ruddle, F.H. Genetic transformation of mouse embryos by microinjection of purified DNA. Proc Natl Acad Sci USA. 1980;77(12): 7380-7384.

Gray, I. C., Campbell, D. A., & Spurr, N. K. (2000). Single nucleotide polymorphisms as tools in human genetics. *Human Molecular Genetics, 9*(16), 2403-2408. doi: 10.1093/hmg/9.16.2403

Gray, J., & Ross, M. E. (2011). Neural Tube Closure in Mouse Whole Embryo Culture. *Journal of Visualized Experiments : JoVE*(56), 3132. doi: 10.3791/3132

Greenstein, J. S., & Foley, R. C. (1957). Early Embryology of the Cow. I. Gastrula and Primitive Streak Stages. *Journal of Dairy Science, 41*(3), 409-421. doi: 10.3168/jds.S0022-0302(58)90934-2

Grupe, A., Li, Y., Rowland, C., Nowotny, P., Hinrichs, A. L., Smemo, S., . . . Goate, A. (2006). A Scan of Chromosome 10 Identifies a Novel Locus Showing Strong Association with Late-Onset Alzheimer Disease. *American Journal of Human Genetics, 78*(1), 78-88.

Haber, J. E. (2000). Partners and pathways: repairing a double-strand break. *Trends in Genetics, 16*(6), 259-264. doi: http://dx.doi.org/10.1016/S0168-9525(00)02022-9

Harris, M. J., & Juriloff, D. M. (2007). Mouse mutants with neural tube closure defects and their role in understanding human neural tube defects. *Birth Defects Research Part A: Clinical and Molecular Teratology, 79*(3), 187-210. doi: 10.1002/bdra.20333

Harris, M. J., & Juriloff, D. M. (2010). An update to the list of mouse mutants with neural tube closure defects and advances toward a complete genetic perspective of neural tube closure. *Birth Defects Research Part A: Clinical and Molecular Teratology, 88*(8), 653-669.

Hau, J. (2008). Animal Models for Human Diseases. In P. M. Conn (Ed.), *Sourcebook of Models for Biomedical Research* (pp. 3-8). Totowa, NJ: Humana Press.

Hentze, M. W., & Kulozik, A. E. (1999). A Perfect Message: RNA Surveillance and Nonsense-Mediated Decay. *Cell, 96*(3), 307-310. doi: http://dx.doi.org/10.1016/S0092-8674(00)80542-5

Herrero, J., Muffato, M., Beal, K., Fitzgerald, S., Gordon, L., Pignatelli, M., . . . Flicek, P. (2016). Ensembl comparative genomics resources. *Database, 2016*. doi: 10.1093/database/bav096

Hogan, B., Costantini, F., & Lacy, E. (1994). *Manipulating the mouse embryo: a laboratory manual* (Vol. 500): Cold Spring Harbor Laboratory Press Cold Spring Harbor, NY.

Hoskins, R. A., Phan, A. C., Naeemuddin, M., Mapa, F. A., Ruddy, D. A., Ryan, J. J., . . . Ellis, M. C. (2001). Single Nucleotide Polymorphism Markers for Genetic Mapping in Drosophila melanogaster. *Genome Research, 11*(6), 1100-1113. doi: 10.1101/gr.178001

Jacobson, M. D., Weil, M., & Raff, M. C. (1997). Programmed Cell Death in Animal Development. *Cell, 88*(3), 347-354. doi: http://dx.doi.org/10.1016/S0092-8674(00)81873-5

Jaenisch, R., & Mintz, B. (1974). Simian Virus 40 DNA Sequences in DNA of Healthy Adult Mice Derived from Preimplantation Blastocysts Injected with Viral DNA. *Proceedings of the National Academy of Sciences of the United States of America, 71*(4), 1250-1254.

Jiang, J., & Struhl, G. (1998). Regulation of the Hedgehog and Wingless signalling pathways by the F-box/WD40-repeat protein Slimb. [10.1038/35154]. *Nature, 391*(6666), 493-496.

Kawakami, K., Amsterdam, A., Shimoda, N., Becker, T., Mugg, J., Shima, A., & Hopkins, N. (2000). Proviral insertions in the zebrafish hagoromo gene, encoding an F-box/WD40-repeat protein, cause stripe pattern anomalies. *Current Biology, 10*(8), 463-466. doi: http://dx.doi.org/10.1016/S0960-9822(00)00444-9

King, G. J., Atkinson, B. A., & Robertson, H. A. (1980). Development of the bovine placentome from Days 20 to 29 of gestation. *Journal of Reproduction and Fertility, 59*(1), 95-100. doi: 10.1530/jrf.0.0590095

Lambert, R. (2007). Breeding strategies for maintaining colonies of laboratory mice: A Jackson Laboratory resource manual. *Jackson Laboratories, 10*. Retrieved from ko.cwru.edu/info/breeding_strategies_manual.pdf

Lecker, S. H., Goldberg, A. L., & Mitch, W. E. (2006). Protein Degradation by the Ubiquitin–Proteasome Pathway in Normal and Disease States. *Journal of the American Society of Nephrology, 17*(7), 1807-1819. doi: 10.1681/asn.2006010083

Li, L., Zheng, P., & Dean, J. (2010). Maternal control of early mouse development. *Development (Cambridge, England), 137*(6), 859-870. doi: 10.1242/dev.039487

Lieber, M. R. (2008). The Mechanism of Human Nonhomologous DNA End Joining. *Journal of Biological Chemistry, 283*(1), 1-5. doi: 10.1074/jbc.R700039200

Lindner, G. M., & Wright, R. W. (1983). Bovine embryo morphology and evaluation. *Theriogenology, 20*(4), 407-416. doi: http://dx.doi.org/10.1016/0093-691X(83)90201-7

Litt, M., & Luty, J. A. (1989). A hypervariable microsatellite revealed by in vitro amplification of a dinucleotide repeat within the cardiac muscle actin gene. *American Journal of Human Genetics, 44*(3), 397-401.

Ma, D., & Liu, F. (2015). Genome Editing and Its Applications in Model Organisms. *Genomics, Proteomics & Bioinformatics, 13*(6), 336-344. doi: http://dx.doi.org/10.1016/j.gpb.2015.12.001

Maddox-Hyttel, P., Alexopoulos, N., Vajta, G., Lewis, I., Rogers, P., Cann, L., . . . Trounson, A. (2003). Immunohistochemical and ultrastructural characterization of the initial post-hatching development of bovine embryos. *Reproduction, 125*(4), 607-623. doi: 10.1530/rep.0.1250607

Maeder, M. L., & Gersbach, C. A. (2016). Genome-editing Technologies for Gene and Cell Therapy. [Review]. *Molecular Therapy*. doi: 10.1038/mt.2016.10

Mao, Z., Bozzella, M., Seluanov, A., & Gorbunova, V. (2008). DNA repair by nonhomologous end joining and homologous recombination during cell cycle in human cells. *Cell cycle 7*(18), 2902-2906.

Marikawa, Y., & Alarcón, V. B. (2009). Establishment of trophectoderm and inner cell mass lineages in the mouse embryo. *Molecular reproduction and development, 76*(11), 1019-1032. doi: 10.1002/mrd.21057

Massa, V., Savery, D., Ybot-Gonzalez, P., Ferraro, E., Rongvaux, A., Cecconi, F., . . . Copp, A. J. (2009). Apoptosis is not required for mammalian neural tube closure. *Proceedings of the National Academy of Sciences of the United States of America, 106*(20), 8233-8238. doi: 10.1073/pnas.0900333106

McClellan, J., & King, M.-C. (2010). Genetic Heterogeneity in Human Disease. *Cell, 141*(2), 210-217. doi: http://dx.doi.org/10.1016/j.cell.2010.03.032

McIlwain, D. R., Berger, T., & Mak, T. W. (2013). Caspase Functions in Cell Death and Disease. *Cold Spring Harbor Perspectives in Biology, 5*(4). doi: 10.1101/cshperspect.a008656

Melina, R. (2010). Why do Medical Researchers Use Mice? Retrieved from http://www.livescience.com/32860-why-do-medical-researchers-use-mice.html

Miko, I. (2008). Thomas Hunt Morgan and Sex Linkage. *Nature Education*, 1(1):143. Retrieved from http://www.nature.com/scitable/topicpage/thomas-hunt-morgan-and-sex-linkage-452

Morriss-Kay, G., Wood, H., & Chen, W.-H. (2007). Normal Neurulation in Mammals. 51-69. Retrieved from http://dx.doi.org/10.1002/9780470514559.ch4 doi:10.1002/9780470514559.ch4

Moscou, M. J., & Bogdanove, A. J. (2009). A Simple Cipher Governs DNA Recognition by TAL Effectors. *Science, 326*(5959), 1501-1501. doi: 10.1126/science.1178817

Muirhead, T. L., Pack, L., & Radtke, C. L. (2014). Unilateral notomelia in a newborn Holstein calf. *The Canadian Veterinary Journal, 55*(7), 659-662.

Murdoch, J. N., Damrau, C., Paudyal, A., Bogani, D., Wells, S., Greene, N. D. E., . . . Copp, A. J. (2014). Genetic interactions between planar cell polarity genes cause diverse neural tube defects in mice. [10.1242/dmm.016758]. *Disease Models and Mechanisms, 7*(10), 1153-1163.

Neer, E. J., Schmidt, C. J., Nambudripad, R., & Smith, T. F. (1994). The ancient regulatory-protein family of WD-repeat proteins. [10.1038/371297a0]. *Nature, 371*(6495), 297-300.

Norrgard, K. (2008). Genetic Variation and Disease: GWAS. *Nature Education*, 87. Retrieved from http://www.nature.com/scitable/topicpage/genetic-variation-and-disease-gwas-682

Oppenheim, R. W., & Haverkamp, L. (1986). Early Development of Behavior and the Nervous System. In E. M. Blass (Ed.), *Developmental Psychobiology and Developmental Neurobiology* (pp. 1-33). Boston, MA: Springer US.

Palis, J. (2006). Yolk Sac Development in Mice *Hematopoietic Stem Cell Development* (pp. 62-71). Boston, MA: Springer US.

Pavletich, N., & Pabo, C. (1991). Zinc finger-DNA recognition: crystal structure of a Zif268-DNA complex at 2.1 A. *Science, 252*(5007), 809-817. doi: 10.1126/science.2028256

Peifer, M., Orsulic, S., Sweeton, D., & Wieschaus, E. (1993). A role for the Drosophila segment polarity gene armadillo in cell adhesion and cytoskeletal integrity during oogenesis. *Development, 118*(4), 1191-1207.

Perez-Pinera, P., Ousterout, D. G., & Gersbach, C. A. (2012). Advances in Targeted Genome Editing. *Current Opinion in Chemical Biology, 16*(3-4), 268-277. doi: 10.1016/j.cbpa.2012.06.007

Powell, W., Morgante, M., Andre, C., Hanafey, M., Vogel, J., Tingey, S., & Rafalski, A. (1996). The comparison of RFLP, RAPD, AFLP and SSR (microsatellite) markers for germplasm analysis. [journal article]. *Molecular Breeding, 2*(3), 225-238. doi: 10.1007/bf00564200

Pruett-Miller, S. M. (2015). *Chromosomal Mutagenesis* (2 ed.).

Pruitt, K. D., Brown, G. R., Hiatt, S. M., Thibaud-Nissen, F., Astashyn, A., Ermolaeva, O., . . . Ostell, J. M. (2014). RefSeq: an update on mammalian reference sequences. *Nucleic Acids Research, 42*(Database issue), D756-D763. doi: 10.1093/nar/gkt1114

Purves, D., Augustine, G., Fitzpatrick, D., & et al. (2001). *Neuroscience*. Sunderland (MA): Sinauer Associates.

Ran, F. A., Hsu, P. D., Wright, J., Agarwala, V., Scott, D. A., & Zhang, F. (2013). Genome engineering using the CRISPR-Cas9 system. [Protocol]. *Nat. Protocols, 8*(11), 2281-2308. doi: 10.1038/nprot.2013.143. http://www.nature.com/nprot/journal/v8/n11/abs/nprot.2013.143.html#supplementary-information.

Risch, N., & Merikangas, K. (1996). The future of genetic studies of complex human diseases. *Science, 273*(5281), 1516-1517.

Roa, A. C., Chavarriaga-Aguirre, P., Duque, M. C., Maya, M. M., Bonierbale, M. W., Iglesias, C., & Tohme, J. (2000). Cross-species amplification of cassava (Manihot esculenta)

(Euphorbiaceae) microsatellites: allelic polymorphism and degree of relationship. *American Journal of Botany, 87*(11), 1647-1655.

Sadler, T. W. (1978). Distribution of surface coat material on fusing neural folds of mouse embryos during neurulation. *The Anatomical Record, 191*(3), 345-349. doi: 10.1002/ar.1091910307

Sadler, T. W. (2005). Embryology of neural tube development. *American Journal of Medical Genetics Part C: Seminars in Medical Genetics, 135C*(1), 2-8. doi: 10.1002/ajmg.c.30049

San Filippo, J., Sung, P., & Klein, H. (2008). Mechanism of Eukaryotic Homologous Recombination. *Annual Review of Biochemistry, 77*(1), 229-257. doi: doi:10.1146/annurev.biochem.77.061306.125255

Schlüter, G. (1973). Ultrastructural observations on cell necrosis during formation of the neural tube in mouse embryos. [journal article]. *Zeitschrift für Anatomie und Entwicklungsgeschichte, 141*(3), 251-264. doi: 10.1007/bf00519046

Schoenwolf, G. C., & Smith, J. L. (2000). Mechanisms of Neurulation. In R. S. Tuan & C. W. Lo (Eds.), *Developmental Biology Protocols: Volume II* (pp. 125-134). Totowa, NJ: Humana Press.

Shea, K., & Geijsen, N. (2007). Dissection of 6.5 dpc Mouse Embryos. *Journal of Visualized Experiments : JoVE*(2), 160. doi: 10.3791/160

Shultz, L. (2016). Why Mouse Genetic Retrieved 02 February, 2016, from https://www.jax.org/genetics-and-healthcare/genetics-and-genomics/why-mouse-genetics#

Silver, L. M., & Barsh, G. S. (1995). Mouse Genetics: *Concepts and Applications* Vol. 60. Retrieved from http://www.informatics.jax.org/silver/index.shtml

Singh, S., & Ganesh, S. (2009). Lafora progressive myoclonus epilepsy: A meta-analysis of reported mutations in the first decade following the discovery of the EPM2A and NHLRC1 genes. *Human Mutation, 30*(5), 715-723. doi: 10.1002/humu.20954

Slack, F. J., & Ruvkun, G. (1998). A novel repeat domain that is often associated with RING finger and B-box motifs. *Trends in Biochemical Sciences, 23*(12), 474-475. doi: http://dx.doi.org/10.1016/S0968-0004(98)01299-7

Smith, C.M., Finger, J.H., Hayamizu, T.F., McCright, I.J., Xu, J., Berghout, J., Campbell, J., Corbani, L.E., Forthofer, K.L., Frost, P.J., Miers, D., Shaw, D.R., Stone, K.R., Eppig, J.T., Kadin, J.A., Richardson, J.E., Ringwald, M. 2014. The mouse Gene Expression Database (GXD): 2014 update. Nucleic Acids Res. 2014 42(D1):D818-D824.

Sonoda, E., Hochegger, H., Saberi, A., Taniguchi, Y., & Takeda, S. (2006). Differential usage of non-homologous end-joining and homologous recombination in double strand break repair. *DNA Repair, 5*(9–10), 1021-1029. doi: http://dx.doi.org/10.1016/j.dnarep. 2006.05.022

Spencer, G. (2002). Background on Mouse as a Model Organism. Retrieved from Genome.Gov website: https://www.genome.gov/10005834

Sturtevant, A. H. (1913). The linear arrangement of six sex-linked factors in Drosophila, as shown by their mode of association. *Journal of Experimental Zoology, 14*(1), 43-59. doi: 10.1002/jez.1400140104

Sutherland, A. (2003). Mechanisms of implantation in the mouse: differentiation and functional importance of trophoblast giant cell behavior. *Developmental Biology, 258*(2), 241-251. doi: http://dx.doi.org/10.1016/S0012-1606(03)00130-1

Takaoka, K., & Hamada, H. (2012). Cell fate decisions and axis determination in the early mouse embryo. *Development, 139*(1), 3-14. doi: 10.1242/dev.060095

Takata, M., Sasaki, M. S., Sonoda, E., Morrison, C., Hashimoto, M., Utsumi, H., . . . Takeda, S. (1998). Homologous recombination and non-homologous end-joining pathways of DNA double-strand break repair have overlapping roles in the maintenance of chromosomal integrity in vertebrate cells. *The EMBO Journal, 17*(18), 5497-5508. doi: 10.1093/emboj/17.18.5497

The Interactive Fly. (2000). Supernumerary Limbs. Available from sdbonline.org The interactive fly Retrieved 02 February 2016, from Society for Developmental Biology http://www.sdbonline.org/sites/fly/dbzhnsky/slimb1.htm

The Jackson Laboratory. Also Known As: FVB, Friend Virus B NIH Jackson Retrieved 02 February, 2016, from https://www.jax.org/strain/001800

Theodosiou, N. A., Zhang, S., Wang, W. Y., & Xu, T. (1998). slimb coordinates wg and dpp expression in the dorsal-ventral and anterior-posterior axes during limb development. *Development, 125*(17), 3411-3416.

Thomas, K. R., Folger, K. R., & Capecchi, M. R. (1986). High frequency targeting of genes to specific sites in the mammalian genome. *Cell, 44*(3), 419-428. doi: http://dx.doi.org/10.1016/0092-8674(86)90463-0

Udan, R. S., & Dickinson, M. E. (2010). Chapter 19 - Imaging Mouse Embryonic Development. In M. W. Paul & M. S. Philippe (Eds.), *Methods in Enzymology* (Vol. Volume 476, pp. 329-349): Academic Press.

Upadhyay, M., Gupta, S., Bhadauriya, P., & Ganesh, S. (2015). Lafora disease proteins laforin and malin negatively regulate the HIPK2-p53 cell death pathway. *Biochemical and*

Biophysical Research Communications, 464(1), 106-111. doi: http://dx.doi.org/10.1016/j.bbrc.2015.06.018

Urnov, F. D., Miller, J. C., Lee, Y.-L., Beausejour, C. M., Rock, J. M., Augustus, S., . . . Holmes, M. C. (2005). Highly efficient endogenous human gene correction using designed zinc-finger nucleases. [10.1038/nature03556]. *Nature, 435*(7042), 646-651. doi: http://www.nature.com/nature/journal/v435/n7042/suppinfo/nature03556_S1.html

Visscher, P.M., Brown, M.A., McCarthy, M.I., & Yang, J. (2012). Five Years of GWAS Discovery. *American Journal of Human Genetics*, *90*(1), 7-24. doi: 10.1016/j.ajhg.2011.11.029

Wallingford, J. B., & Harland, R. M. (2002). Neural tube closure requires Dishevelled-dependent convergent extension of the midline. *Development*, *129*(24), 5815-5825. doi: 10.1242/dev.00123

Wallingford, J. B., Niswander, L. A., Shaw, G. M., & Finnell, R. H. (2013). The Continuing Challenge of Understanding, Preventing, and Treating Neural Tube Defects. *Science, 339*(6123). doi: 10.1126/science.1222002

Wang, H., & Dey, S. K. (2006). Roadmap to embryo implantation: clues from mouse models. [10.1038/nrg1808]. *Nat Rev Genet, 7*(3), 185-199. doi: http://www.nature.com/nrg/journal/v7/n3/suppinfo/nrg1808_S1.html

Waters, K. (2013). What's Going On In There: Fetal Development of the Beef Cow. Retrieved from iGrow.Org website: http://igrow.org/livestock/beef/whats-going-on-in-there-fetal-development-of-the-beef-calf/

Weber, J. L., & May, P. E. (1989). Abundant class of human DNA polymorphisms which can be typed using the polymerase chain reaction. *American Journal of Human Genetics, 44*(3), 388-396.

Weil, M., Jacobson, M. D., & Raff, M. C. (1997). Is programmed cell death required for neural tube closure? *Current Biology, 7*(4), 281-284. doi: http://dx.doi.org/10.1016/S0960-9822(06)00125-4

Wojcik, E. J., Glover, D. M., & Hays, T. S. (2000). The SCF ubiquitin ligase protein Slimb regulates centrosome duplication in Drosophila. *Current Biology, 10*(18), 1131-1134. doi: http://dx.doi.org/10.1016/S0960-9822(00)00703-X

Wright, David A., Li, T., Yang, B., & Spalding, Martin H. (2014). TALEN-mediated genome editing: prospects and perspectives. [10.1042/BJ20140295]. *Biochemical Journal, 462*(1), 15-24.

Wu, Y., Liang, D., Wang, Y., Bai, M., Tang, W., Bao, S., . . . Li, J. (2013). Correction of a Genetic Disease in Mouse via Use of CRISPR-Cas9. *Cell Stem Cell, 13*(6), 659-662. doi: http://dx.doi.org/10.1016/j.stem.2013.10.016

Yamaguchi, Y., & Miura, M. (2013). How to form and close the brain: insight into the mechanism of cranial neural tube closure in mammals. *Cellular and Molecular Life Sciences, 70*(17), 3171-3186. doi: 10.1007/s00018-012-1227-7

Zhang, S., Lin, H., Kong, S., Wang, S., Wang, H., Wang, H., & Armant, D. R. (2013). Physiological and molecular determinants of embryo implantation. *Molecular aspects of medicine, 34*(5), 939-980. doi: 10.1016/j.mam.2012.12.011

Zietkiewicz, E., Rafalski, A., & Labuda, D. (1994). Genome Fingerprinting by Simple Sequence Repeat (SSR)-Anchored Polymerase Chain Reaction Amplification. *Genomics, 20*(2), 176-183. doi: http://dx.doi.org/10.1006/geno.1994.1151

Zohn, I. E., & Sarkar, A. A. (2008). Chapter 1 Modeling Neural Tube Defects in the Mouse *Current Topics in Developmental Biology* (Vol. Volume 84, pp. 1-35): Academic Press.

Appendix A: Appendix Tables

Table A.1 Gene-Edited Founder FVB Mice Received From Cyagen

Gene-edited Founder Mice From Cyagen				
Mouse ID	Sex	Genotype	Generation	DOB
#70	F	-19 bp heterozygous	F0	8-Apr-14
#48	M	-2 bp heterozygous	F0	8-Apr-14
#60	M	-12 bp heterozygous	F0	8-Apr-14
#7	F	-2 bp heterozygous	F1 (#48 x WT)	24-Jun-14
#2	M	-2 bp heterozygous	F1 (#48 x WT)	24-Jun-14
#4	M	-2 bp heterozygous	F1 (#48 x WT)	24-Jun-14
#3	F	-12 bp heterozygous	F1 (#60 x WT)	27-Jun-14
#14	F	-12 bp heterozygous	F1 (#60 x WT)	27-Jun-14
#5	M	-12 bp heterozygous	F1 (#60 x WT)	27-Jun-14
#8	M	-12 bp heterozygous	F1 (#60 x WT)	27-Jun-14
#7	F	-19 bp heterozygous	F1 (#70 x WT)	27-Jun-14
#6	M	-19 bp heterozygous	F1 (#70 x WT)	27-Jun-14

Table A.2 Genotype and Sex Distribution of Litters by Mating Type

WT x -19 bp Heterozygous						
	Genotype (Dead at Birth)		Sex			
Dam	WT	Heterozygous	M	F	Litter Size	DOB
#9	7(0)	3(1)	4	6	11	25-Jan-15
#14	3(0)	4(0)	6	1	7	25-Jan-15
#10	7(0)	3(1)	5	5	11	31-Jan-15
#10	7(0)	4(0)	5	6	11	3-Apr-15
#53	3(1)	5(0)	1	7	9	11-May-15
#33	3(0)	5(0)	4	4	8	18-Jun-15
#53	4(0)	3(0)	3	4	7	6-Jul-15
#162	4(0)	5(1)	2	7	10	6-Jul-15
Total	38(1)	32(3)	30	40	74	

WT x -12 bp Heterozygous						
	Genotype (Dead at Birth)		Sex			
Dam	WT	Heterozygous	M	F	Litter Size	DOB
#6	7(0)	4(0)	4	3	11	31-Jan-15
#22	6(0)	3(0)	4	3	9	3-Feb-15
#23	4(0)	3(1)	2	5	8	3-Feb-15
#21	3(1)	3(0)	2	5	7	8-Feb-15
#7	5(0)	3(0)	4	4	8	26-Feb-15
#38	3(0)	4(0)	2	5	7	18-Jun-15
#204	2(0)	3(0)	2	3	5	18-Sep-15
#375	5(0)	2(0)	3	4	7	21-Sep-15
#363	5(0)	4(1)	6	3	10	21-Sep-15
#373	2(0)	7(0)	4	5	9	21-Sep-15
#51	0(4)	0(5)	0	0	9	21-Sep-15
#399	4(0)	4(0)	7	1	8	27-Dec-15
#403	4(0)	2(0)	3	3	6	28-Dec-15
Total	50(5)	42(7)	43	44	104	

Table A.2 (Cont.)

WT x -2 bp Heterozygous						
	Genotype (Dead at Birth)		Sex			
Dam	WT	Heterozygous	M	F	Litter Size	DOB
#17	4(0)	4(0)	4	4	8	27-Jan-15
#19	4(0)	5(0)	6	3	9	27-Jan-15
#20	1(1)	5(2)	2	4	9	27-Jan-15
#24	3(0)	4(0)	4	3	7	8-Jul-15
#23	6(1)	1(0)	4	3	8	11-Jul-15
#199	4(0)	3(1)	3	4	8	11-Jul-15
#291	5(1)	3(2)	2	6	11	21-Sep-15
#292	4(1)	2(2)	4	2	9	21-Sep-15
#344	4(0)	5(0)	1	8	9	21-Sep-15
#346	4(0)	7(0)	4	7	11	21-Sep-15
Total	39(4)	39(7)	34	44	89	

-19 bp Heterozygous x -19 Heterozygous						
	Genotype (Dead at Birth)		Sex			
Dam	WT	Heterozygous	M	F	Litter Size	DOB
#18	1(0)	4(1)	1	4	6	30-Mar-15
#45	5(0)	6(0)	3	8	11	3-May-15
#27	2(0)	6(2)	4	4	10	4-May-15
#43	3(0)	5(0)	3	5	8	7-May-15
#29	0(3)	0(1)	0	0	4	11-May-15
#18	4(1)	3(1)	6	1	9	18-May-15
#130	2(0)	7(0)	6	3	9	19-Jun-15
#129	0(1)	0(2)	0	0	3	21-Jun-15
#27	2(0)	5(1)	3	4	8	10-Jul-15
#188	3(0)	5(0)	4	4	8	8-Jul-15
#468	1(0)	9(0)	6	4	10	14-Feb-16
#346	0(3)	0(1)	0	0	4	17-Feb-16
Total	23(8)	50(9)	36	37	90	

Table A.2 (Cont.)

-12 bp Heterozygous x -12 bp Heterozygous						
	Genotype (Dead at Birth)		Sex			
Dam	WT	Heterozygous	M	F	Litter Size	DOB
#8	0(2)	2(1)	2	0	5	31-Jan-15
#51	2(0)	3(0)	2	3	5	6-Apr-15
#116	1(0)	1(0)	1	1	2	14-Apr-15
#114	2(0)	6(0)	3	5	8	15-Apr-15
#122	4(0)	5(0)	4	5	9	4-May-15
#50	1(0)	0(6)	0	1	7	13-May-15
#54	3(0)	2(0)	2	3	5	13-May-15
#51	1(0)	4(0)	0	5	5	21-May-15
#119	4(0)	4(0)	5	3	8	21-May-15
#50	1(0)	3(0)	3	1	4	6-Jul-15
#51	2(0)	4(1)	3	3	7	6-Jul-15
#54	2(1)	3(0)	2	3	6	17-Jul-15
#238	1(0)	3(0)	2	2	4	17-Jul-15
#253	3(0)	4(0)	4	3	7	9-Aug-15
#206	6(0)	5(0)	6	5	11	22-Aug-15
#253	2(0)	5(3)	4	2	10	20-Sep-15
#257	3(0)	8(0)	9	2	11	23-Sep-15
Total	38(3)	62(11)	52	47	114	

Table A.2 (Cont.)

-2 bp Heterozygous x -2 bp Heterozygous						
	Genotype (Dead at Birth)		Sex			
Dam	WT	Heterozygous	M	F	Litter Size	DOB
#12	0(0)	0(2)	0	0	2	3-Feb-15
#25	0(0)	8(0)	5	3	8	1-Apr-15
#47	1(0)	2(0)	0	3	3	11-May-15
#37	2(0)	2(0)	2	2	4	13-May-15
#25	1(0)	4(0)	1	4	5	16-May-15
#135	2(0)	3(2)	3	2	7	19-Jun-15
#148	0(0)	3(0)	2	1	3	7-Jul-15
#149	2(0)	6(0)	4	4	8	11-Jul-15
#326	3(0)	4(0)	4	3	7	16-Sep-15
#328	1(0)	4(0)	1	4	5	17-Sep-15
#329	1(0)	4(1)	4	1	6	17-Sep-15
#298	5(0)	4(0)	8	1	9	17-Sep-15
#325	0(0)	1(1)	1	0	2	23-Sep-15
#327	0(0)	6(0)	3	3	6	14-Feb-16
#500	2(0)	4(0)	3	3	6	16-Feb-16
#329	0(1)	0(0)	0	0	1	16-Feb-16
#329	2(0)	4(0)	1	5	6	23-Mar-16
Total	22(1)	61(4)	42	39	88	

Table A.3 Two Sample T-Tests Assuming Equal Variance Comparing Litter Sizes by Mating Type

	-19 bp x -19 bp	-12 bp x -12 bp
Mean	7.5	6.7
Variance	7	6.6
Observations	12	17
Pooled Variance	6.8	
Hypothesized Mean Difference	0	
df	27	
t Stat	0.81	
P(T<=t) two-tail	0.42	
t Critical two-tail	2.05	

	-19 bp x -19 bp	-2 bp x -2 bp
Mean	7.5	5.2
Variance	7	5.5
Observations	12	17
Pooled Variance	6.1	
Hypothesized Mean Difference	0	
df	27	
t Stat	2.49	
P(T<=t) two-tail	0.02	
t Critical two-tail	2.05	

Table A.3 (cont.)

	-12 bp x -12 bp	-2 bp x -2 bp
Mean	6.7	5.2
Variance	6.6	5.5
Observations	17	17
Pooled Variance	6.1	
Hypothesized Mean Difference	0	
df	32	
t Stat	1.81	
P(T<=t) two-tail	0.08	
t Critical two-tail	2.04	

	WT x -19 bp	WT x -12 bp
Mean	8.9	8.0
Variance	1.7	2.7
Observations	10.0	13.0
Pooled Variance	2.2	
Hypothesized Mean Difference	0	
df	21	
t Stat	1.43	
P(T<=t) two-tail	0.17	
t Critical two-tail	2.08	

Table A.3 (cont.)

	WT x -19 bp	WT x -2 bp
Mean	8.9	9.3
Variance	1.7	3.1
Observations	10	8
Pooled Variance	2.3	
Hypothesized Mean Difference	0	
df	16	
t Stat	-0.49	
P(T<=t) two-tail	0.63	
t Critical two-tail	2.12	

t-Test: Two-Sample Assuming Equal Variances

	WT x -12 bp	WT x -2 bp
Mean	8.0	9.3
Variance	2.7	3.1
Observations	13	8
Pooled Variance	2.8	
Hypothesized Mean Difference	0	
df	19	
t Stat	-1.66	
P(T<=t) two-tail	0.11	
t Critical two-tail	2.09	

Appendix Table A.4 Chi Square Analysis by Mating Type

WT x -19 bp								
Genotype	Observed	%	Expected	%	O-E	$(O-E)^2$	$(O-E)^2/E$	P Value
WT	43.00	0.48	44.50	0.50	-1.50	2.25	0.05	0.75
Heterozygous	46.00	0.52	44.50	0.50	1.50	2.25	0.05	
Homozygous Recessive	0.00	0.00	0.00	0.00	0.00	0.00	0.00	
Total	89.00		89.00			Chi^2	0.10	

WT x -12 bp								
Genotype	Observed	%	Expected	%	O-E	$(O-E)^2$	$(O-E)^2/E$	P Value
WT	55.00	0.53	52.00	0.50	3.00	9.00	0.17	0.55
Heterozygous	49.00	0.47	52.00	0.50	-3.00	9.00	0.17	
Homozygous Recessive	0.00	0.00	0.00	0.00	0.00	0.00	0.00	
Total	104.00		104.00			Chi^2	0.35	

WT x -2 bp								
Genotype	Observed	%	Expected	%	O-E	$(O-E)^2$	$(O-E)^2/E$	P Value
WT	39.00	0.53	37.00	0.50	2.00	4.00	0.11	0.64
Heterozygous	35.00	0.47	37.00	0.50	-2.00	4.00	0.11	
Homozygous Recessive	0.00	0.00	0.00	0.00	0.00	0.00	0.00	
Total	74.00		74.00			Chi^2	0.22	

Table A.4 (cont.)

-19 bp x -19 bp								
Genotype	Observed	%	Expected	%	O-E	$(O-E)^2$	$(O-E)^2/E$	P Value
WT	31.00	0.34	22.50	0.25	8.50	72.25	3.21	<0.01
Heterozygous	59.00	0.66	45.00	0.50	14.00	196.00	4.36	
Homozygous Recessive	0.00	0.00	22.50	0.25	-22.50	506.25	22.50	
Total	90.00		90.00			Chi^2	30.07	

-12 bp x -12 bp								
Genotype	Observed	%	Expected	%	O-E	$(O-E)^2$	$(O-E)^2/E$	P Value
WT	41.00	0.36	28.50	0.25	12.50	156.25	5.48	<0.01
Heterozygous	73.00	0.64	57.00	0.50	16.00	256.00	4.49	
Homozygous Recessive	0.00	0.00	28.50	0.25	-28.50	812.25	28.50	
Total	114.00		114.00			Chi^2	38.47	

-12 bp x -12 bp (E8.5)								
Genotype	Observed	%	Expected	%	O-E	$(O-E)^2$	$(O-E)^2/E$	P Value
WT	10.00	0.40	6.25	0.25	3.75	14.06	2.25	0.01
Heterozygous	15.00	0.60	12.50	0.50	2.50	6.25	0.50	
Homozygous Recessive	0.00	0.00	6.25	0.25	-6.25	39.06	6.25	
Total	25.00		25.00			Chi^2	9.00	

-2 bp x -2 bp								
Genotype	Observed	%	Expected	%	O-E	$(O-E)^2$	$(O-E)^2/E$	P Value
WT	23.00	0.26	22.00	0.25	1.00	1.00	0.05	<0.01
Heterozygous	65.00	0.74	44.00	0.50	21.00	441.00	10.02	
Homozygous Recessive	0.00	0.00	22.00	0.25	-22.00	484.00	22.00	
Total	88.00		88.00			Chi^2	32.07	

Table A.5 Chi Square Analysis for Lethal Inheritance by Mating Type

-19 bp x -19 bp								
Genotype	Observed	%	Expected	%	O-E	$(O-E)^2$	$(O-E)^2/E$	P Value
WT	31.00	0.34	29.70	0.33	1.30	1.69	0.06	0.78
Heterozygous	59.00	0.66	60.30	0.67	1.30	1.69	0.03	
Homozygous Recessive	0.00	0.00	0.00	0.00	0.00	0.00	0.00	
Total	90.00		90.00			Chi^2	0.08	

-12 bp x -12 bp								
Genotype	Observed	%	Expected	%	O-E	$(O-E)^2$	$(O-E)^2/E$	P Value
WT	41.00	0.36	37.62	0.33	3.38	11.42	0.30	0.50
Heterozygous	73.00	0.64	76.38	0.67	3.38	11.42	0.15	
Homozygous Recessive	0.00	0.00	0.00	0.00	0.00	0.00	0.00	
Total	114.00		114.00			Chi^2	0.45	

-12 bp x -12 bp (E8.5)								
Genotype	Observed	%	Expected	%	O-E	$(O-E)^2$	$(O-E)^2/E$	P Value
WT	10.00	0.40	8.25	0.33	1.75	3.06	0.37	0.46
Heterozygous	15.00	0.60	16.75	0.67	1.75	3.06	0.18	
Homozygous Recessive	0.00	0.00	0.00	0.00	0.00	0.00	0.00	
Total	25.00		25.00			Chi^2	0.55	

-2 bp x -2 bp								
Genotype	Observed	%	Expected	%	O-E	$(O-E)^2$	$(O-E)^2/E$	P Value
WT	23.00	0.26	29.04	0.33	6.04	36.48	1.26	0.17
Heterozygous	65.00	0.74	58.96	0.67	6.04	36.48	0.62	
Homozygous Recessive	0.00	0.00	0.00	0.00	0.00	0.00	0.00	
Total	88.00		88.00			Chi^2	1.88	